Drift velocity partitioning indicates anomalous high velocities for the Indian plate during ~65 Ma

Amarjeet Ramesh Bhagat[1,1], S J Sangode[1,1], Ashish Dongre[1], and Ashish Dongre[1]

[1]Savitribai Phule Pune University

November 30, 2022

Abstract

A rapid northward drift of the Indian plate after 130 Ma has also recorded significant plate rotations due to the torques resulting from multiple vectorial forces. Magnetic anomaly, seismic tomography and palaeomagnetic database is used here to constrain drift velocities, tilt and lithospheric root delamination at different temporal snapshots. It results into estimates of 263.2 to 255.7 mmyr^{-1} latitudinal drift, 234 to 227.3 mmyr^{-1} longitudinal drift and 352.2 to 342.1 mmyr^{-1} diagonal drift, for the period from ~66 to 64 Ma during the Chrons C30n.y–C29n.y. Alternative models suggest active driving forces arising from *i)* slab pull, *ii)* ridge push from eastern-, western and southern plate margins, and *iii)* Reunion plume-push force; in addition to delamination of the lithospheric root during approximately 65+2 Ma. Delamination amplified the buoyancy of the Indian plate in contrast to sudden loading from Deccan basaltic pile that resulted into complex drift dynamics expressed by hyper plate velocities within global plate circuit.

Drift rate partitioning indicates anomalous high velocities for the Indian plate during ~65 Ma

Amarjeet R. Bhagat[1], S. J. Sangode[1], Ashish Dongre[1]

[1]Department of Geology, Savitribai Phule Pune University, Pune, India

Corresponding author: Satish Sangode (sangode@unipune.ac.in)

Key Points:

- **Very high drift rates for the Indian subcontinent during the Deccan Trap eruption are reported.**
- **Dynamics of the reported drift rates are explained.**
- **Present day location of the lithospheric root delaminated from the Indian subcontinent is proposed.**

Abstract

A rapid northward drift of the Indian plate after 130 Ma has also recorded significant plate rotations due to the torques resulting from multiple vectorial forces. Magnetic anomaly, seismic tomography and palaeomagnetic database is used here to constrain drift velocities, tilt and lithospheric root delamination at different temporal snapshots. It results into estimates of 263.2 to 255.7 mmyr^{-1} latitudinal drift, 234 to 227.3 mmyr^{-1} longitudinal drift and 352.2 to 342.1 mmyr^{-1} diagonal drift, for the period from ~66 to 64 Ma during the Chrons C30n.y–C29n.y. Alternative models suggest active driving forces arising from *i)* slab pull, *ii)* ridge push from eastern-, western and southern plate margins, and *iii)* Reunion plume-push force; in addition to delamination of the lithospheric root during approximately 65$\pm$2 Ma. Delamination amplified the buoyancy of the Indian plate in contrast to sudden loading from Deccan basaltic pile that resulted into complex drift dynamics expressed by hyper plate velocities within global plate circuit.

Plain Language Summary:

Paleomagnetism has proved indispensable in plate tectonic reconstructions. Often the seafloor spreading rates are calculated from the Marine magnetic anomalies in the ocean basins. However, it is possible that these robust features of the global conveyor belt may at times miss events which are significant in magnitude occurring within a short time span. Here, we present one such event during the Deccan trap eruption. It is well established that the highest plate velocities that can be achieved by drifting plates range around

180-200 mmyr^{-1}. However, in the present study based on paleomagnetic data, we present drift rates that are in excess of 300 mmyr^{-1}, these drift rates result from contemporary existence of multiple plate driving forces that acted on the Indian plate during the K-Pg event. Slab pull combined together with plume push, ridge push and lithospheric root delamination propelled the Indian plate at tremendously high velocities which resulted in multiple course corrections along within a short span of ~1.5 Ma.

Introduction:

The Indian plate presents one of the most dynamic trajectories of plate motion by its rapid northward drifts and clockwise/anticlockwise rotations (Patriat and Acache 1984, Eagles and Hoang 2013, O'Neill et al 2003). Multiple surges in the plate velocities are recorded at 130, 85 and 65 Ma (Van Hinsbergen et al 2011, Eagles and Hoang 2013, Gibbons et al 2013, Gibbons et al 2015, Jagoutz et al 2015, Cande et al 2010, Cande and Stegman 2011, Demets and Merkouriev 2021, Eagles and Wibisono 2013) and are related to Indian plate encounters with three well established mantle plumes. The 130 Ma event was caused by the Kerguelen plume forming the Rajmahal (Kale 2020, Ghatak and Basu 2011, Taludkar and Murthy 1971) traps in India, Bunbury basalts in Australia (Frey et al 1996, Ingle et al 2002, Zhu et al 2009, Olierook et al 2016) and Kerguelen plateau in the Southern Indian Ocean. This resulted in rifting of India from East Gondwana (Aitchison et al 2007, Acharyya 2000, Argus et al 2011, Bardintzeff et al 2010) forming the Indian subcontinental block comprising (India + Madagascar + Seychelles). This rifting was followed by the Marion plume arrival at the End Cretaceous (~90-85Ma) (Torsvik et al 1998, Georgen et al 2001, Storey 1995), resulting in separation of India + Seychelles block from Madagascar.

The final Reunion plume encounter led to India-Seychelles separation and eruption of the Deccan flood basalts at ~65.5 Ma (Sangode et al 2022, Vandamme et al 1991, Jay and Widdowson 2006, Chenet et al 2007, Chenet et al 2008).

Drift, rotation and tilt of the Indian plate

Based on marine magnetic anomaly data it has been established that the Indian subcontinent moved at extreme velocities during the period from C32 to C28 at highest speeds of ~185- 200 mm/yr recorded during Chron C29r (Cande and Stegman 2011, Pusok and Stegman 2020, Sangode et al 2022, Rodriguez et al 2021, Van Hinsbergen et al 2015). These velocities are anomalous when compared with the fastest spreading rates obtained from the East Pacific Rise (~140mm/yr) existing today (Lonsdale 1977, Clennett et al 2020). This high drift velocity for the Indian plate has been classically attributed to its interaction with the Reunion plume and the Deccan eruption event, which amplified the existing rapid velocity of the Indian plate.

Primarily, the drift rates are calculated from the Marine Magnetic Anomalies (MMA) in the ocean basins; however, in situations where anomaly data are

sparse the drift rates are calculated from paleomagnetic measurements based on land values. Present work is built up on the database of Sangode et al (2022), who discovered the Deccan inclination anomaly from a compilation and analysis of existing paleomagnetic data from the Deccan Traps. They discovered that the paleomagnetic inclinations for the chrons C30n, C29r and C29n differ significantly for such a short-time span, with C29r depicting highly anomalous inclination values. This inclination anomaly was attributed to the ~10 tilt of the Indian plate towards north leading to short episode of epicontinental marine transgression along the Narmada rift (Kumari et al 2020, Keller et al 2021). This tilt is attributed to the arrival of the Reunion plume at the NW-W periphery of the Indian subcontinent resulting in uplift of southern tip of peninsular India and dipping of the northern edge of the subcontinent for a very brief time spanning C29r. The tilt was restored back to normal during C29n, resulting in normal inclination values for the same.

Constrains from paleomagnetic database

Statistical analysis of the paleomagnetic data leads to 2 differing results which contrast not only in position but also significantly differ in the drift velocities for the Indian subcontinent. 'Model A' explains the results obtained from Central tendency data, while 'model B' explains the results obtained from the Filtered mean data. As it is not clear when the Deccan volcanism event precisely initiated, we have considered the initial position of the Indian subcontinent for our calculations at the end of Chron C30n while the final position at the end of C29n signifying the end of main phase eruption of Deccan tholeiites. This provides us with a ~1.5 Ma (1.518 Ma for GTS2020; 1.563 for MQSD20) time window to monitor the movements of the Indian subcontinent spanning C29r and C29n. The co-ordinates for Nagpur in Central India were used as a reference point for calculating movement of Indian plate.

For 'model A' (Central tendency data), the D/I value are 333/-38 at C30n.y and 341/-32 at C29n.y. The initial position of the Indian subcontinent at C30n.y is exactly southwest of the final position at C29n.y. This agrees well with the established literature, except for the fact that the displacement of India for the specified time period is massive. The differences in initial and final positions depict a latitudinal drift of 6° and a longitudinal drift of 8°. Simple trigonometric calculations reveal a diagonal drift of about 10° which is colossal when compared with the highest drift rates that have been recorded for India-Eurasia convergence. Assuming 1° = 111 km, latitudinal, longitudinal and diagonal drifts can be calculated as 666 km, 888 km and 1110 km respectively. These results when compared with the above-mentioned timespan, evolve into drift rates which have not been directly documented earlier. These are presented in the Table 2 and figure 3.

'Model B' (Filtered mean data) however indicates an altogether different result. The D/I values are 338/-37.8 and 334.8/-35.1 respectively for the final and initial positions (i.e., C30n.y and C29n.y). This presents smaller drift rates when compared with 'model A'. However, there appears to be some sort of

disparity when analysing the drift directions. The final and initial positions differ in the convergence trend that is generally accepted for India-Eurasia. The subcontinent appears to have moved towards northwest with respect to its initial position at C30n.y. This is in contrast with the results from 'model A' which shows a northeast convergence for the above-mentioned timespan. The drift values calculated from the initial and final positions reveal a 3.6° latitudinal, 3.2° longitudinal and 4.82° diagonal drifts respectively for the 'model B'. These values equate to displacements of 399.6 km, 355.2 km and 534.65 km respectively and are shown in Table 2 and figure 4.

Recent studies have attributed these high drift rates to multiple factors, most prominent being the convergence of India towards Eurasia owing to the multiple subduction zones present at the southern Eurasian margin (Aitchison et al 2000, Aitchison and Davis 2004, Baxter et al 2016, Bouilhol et al 2013, Gibbons et al 2015, Buckman et al 2018). The enormous slab pull experienced by the Indian plate towards north has been postulated by many to be the major driver of rapid movement of India. This could possibly be the case if the lithospheric plate experiencing slab pull was entirely oceanic in character and did not carry a significant continental landmass such as India (Pusok and Stegman 2020, Van Hinsbergen et al 2015, Zahirovic et al 2012). The negative buoyancy of the Indian subcontinent could possibly not have allowed such a high drift rate based merely on slab pull of the downgoing oceanic slab attached to the Indian plate (Forsyth and Uyeda 1975, Morgan and Parmentier 1984).

Slab pull or Ridge push?

Amongst the forces acting on the Indian plate during Late Cretaceous, slab pull appears to be the major driver; as the velocity of a drifting plate is directly proportional to the length of subduction zone attached to it. This is evident as there existed a long subduction zone all along the southern Eurasian margin. This more than ~10,000 km subduction zone would have acted as a major driver for the plate motion of India since its rifting from Madagascar (~85-90 Ma), only to be modified/interrupted by the Reunion plume (67-64 Ma). The western spreading centre being younger would be more vigorous and thereby have a dominant role in driving the Indian plate as compared to the eastern spreading centre during the Late Cretaceous. This coupled together with the push emanating from the southern spreading ridge and the slab pull from the north would have resulted in a northerly – northeasterly drift of the Indian subcontinent.

However, based on the analysis of the Declination data in 'model B', it appears that this dominant drift direction might have been affected severely or it altogether changed although for a short time interval. This implies that a plume head upon interaction with continental lithosphere can significantly affect the directions of plate movement, by overcoming the existing plate driving forces. This is confirmed by the lithospheric tilting recorded within the DVP (Sangode et al 2022), which depicts that the incipient plume push arising from the first interaction of a mantle plume with continental lithosphere can result in tilting

of the continental block. Along with this tilting there appears to be an additional sideways component associated, more likely to result in the sideward drift/slip with velocities that surpass existing plate tectonic speed limits. Thus, the plume push force originating from the Reunion plume not only enhanced the drift velocity of the Indian plate with respect to Eurasia, but it could have also caused a previously unnoticed westward drift/slip for ~1.5 Ma with velocities as high as ~352 mm/yr $^{-1}$.

This is possible as the plume made its first contact along the North-western fringes of the Indian subcontinent thereby resulting in a northward tilting, where maximum part of the subcontinent was positioned. This was followed by a slip towards west along periphery of the plume, where the point of contact between the plume head and subcontinent acted as a pivot thereby rotating the continental block. After C30n.y the subcontinent moved beyond the sphere of direct influence of the plume, restoring the slab pull and ridge push forces resulting in north-eastward drift of India. The drift rates were however significantly enhanced with renewed push from the Reunion plume resulting in the rates that were higher than what they were before the Reunion encounter, but significantly lower than what it was during the event which lasted about 1.5 Ma.

Tomographic hunt for the lost root

Another possible explanation for this rapid drift could be attributed to the absence of a thick cratonic root beneath the Indian subcontinent (Kumar et al 2007, Dessai and Griffin 2021, Jaupart and Mareschal 1999). This can be expected in our case as Indian subcontinent has had 3 major encounters with mantle plumes within less than 70Ma (Dessai and Griffin 2021, Griffin et al 2009, Paul and Ghosh 2021). The multiple encounters could possibly have led to thermal erosion of the continental lithospheric root. The lithospheric roots act as anchors for the continents in the mantle, once removed or lost, it is difficult for the continents to retain the coefficient of friction with the asthenospheric or mantle drag (Stoddard and Abbot 1996). A buoyant continental mass deprived of its root can prove to be an excellent candidate for this continental "MotoGP".

We present surface wave tomographic models along a traverse in the Indian ocean at co-ordinates (25°S, 55°E) and (15°N, 75°E). These models have been derived using Submachine an open-source seismic tomography software. S-wave models provide better resolution in the upper mantle, which explains the choice of our models. The results show a distinct cold-high velocity anomaly at the reunion latitudes in the upper mantle enclosed by lower velocity material highlighted by the dashed enclosures. The shape of this anomaly does not correspond to a subducted slab of oceanic lithosphere, nor there have been any reported subductions at those latitudes in the past 100 Ma. We say 100 Ma as the slab is yet lying in the upper mantle and has not ventured below 1000 km. The horizontal alignment also defies any chances of a subducted slab at such shallow depths in the mantle. Besides the direction of elongation corresponds to that of the movement of the Indian subcontinent. We therefore propose that this could possibly be the delaminated lithospheric root of the Indian subcontinent,

which was removed by the Reunion plume resulting in reduced coupling between the Indian plate and the underlying asthenosphere. This loss of lithosphere effectively increased the efficiency of slab pull experienced by the Indian plate thereby resulting in enhanced velocities followed by the Deccan event.

Based on the above 4 models it appears that bottom of the anomaly lies at depths of 660 km to 710 km barring HMSL-S06 which gives a maximum depth of 535 km. Assuming sinking rates of 10 $mmyr^{-1}$ and 20 $mmyr^{-1}$, the models predict that the outlined anomaly subducted somewhere between 66-33 Ma (3D2016_09Sv), 68-34 Ma (GyPSuM-S), 53.5-26.725 Ma (HMSL-S06) and 71-35.5 Ma (SL2013sv). All of these age ranges except HMSL-S06 closely fit with timing of the Deccan event. Thus, it is highly unlikely, that the occurrence of a cold high-density anomaly exactly around Reunion latitudes with a geometry that does not resemble a subducted lithospheric slab and mantle sinking rates that when backtracked lead to a delamination age of 70-66 Ma, which is precisely the age for Deccan-Reunion event is a mere coincidence. This therefore strengthens the argument that the Indian plate cratonic root was completely removed during the Deccan event. This decoupling led to a decrease in the asthenospheric drag on the Indian plate, which combined with the slab pull and plume push forces resulted in tremendously high velocities.

Conclusions

Paleogeographic reconstruction positions India in close proximity to spreading centres at the western and southern margins before the plume interaction at ~70-65 Ma (Van Hinsbergen et al 2019, Rodriguez et al 2021, Cande and Stegman 2011, Parsons et al 2021). The Indian subcontinent formed less than ~50% (roughly about 35-40%) of the total area of the Indian plate, which was dominantly comprised of oceanic lithosphere. Zahirovic et al (2015), explained based on numerical models that plates with a significant portion of the plate boundary involved in subduction zone experienced higher drift velocities compared to plates with no active subducting margins. If the subducting plate happens to carry a continental block, the size of the block would in turn decide the velocity of the moving plate. From the paleo-reconstructions it is obvious that Indian plate had a massive subduction zone at its northern boundary (Hafkenschied et al 2004, Van der Meer et al 2018, Gibbons et al 2015) thereby placing an active propellant for the plate velocities.

Based on our calculations, we propose that the Indian subcontinent travelled at exceedingly high velocities which had never been recorded earlier directly. The Indian subcontinent experienced a brief pulse of hyper-spreading velocities when it encountered the Reunion plume-head (end of C30n to the end of C29n). The positive buoyancy created by the plume head and the negative buoyancy due to Deccan basalt loading, both appear to have encouraged the larger displacements besides tilting of the continental block by $\sim 10^0$. Once the plate moved away substantially from the plume head, lower velocities facilitated by lithospheric cooling are observed. The torques resulting from the multiple force vectors acting simultaneously are expressed by the clockwise/anticlockwise rotations

and suitably derived from longitudinal and latitudinal drift components of the Indian plate during the same time. Thus, finally we report here one of the highest ever recorded plate velocities although for a short time span resulting from a combination of factors with changing intensities that modified plate movement including the directions precisely at 65$\pm$2 Ma.

Acknowledgements:

Authors acknowledge fellowship and other supports under Ministry of Earth Sciences grant MoES/P.O.(Seismo)/1(353)/2018. Authors acknowledge the Head, Department of Geology, Savitribai Phule Pune University, Pune (India) for permissions and support.

References

Acharyya S.K., (2000). Break Up of Australia-India-Madagascar Block, Opening of the Indian Ocean and Continental Accretion in Southeast Asia With Special Reference to the Characteristics of the Peri-Indian Collision Zones, Gondwana Research, Volume 3, Issue 4, 2000, Pages 425- 43, ISSN 1342-937X, https://doi.org/10.1016/S1342-937X(05)70753-X.

Aitchison, J. C., Ali, J. R., and Davis, A. M. (2007), When and where did India and Asia collide? J. Geophys. Res., 112, B05423, doi:10.1029/2006JB004706.

Aitchison, J.C., Badengzhu, Davis, A.M., Liu, J.B., Luo, H., Malpas, J., McDermid, I.R., Wu, H., Ziabrev, S., & Zhou, M. (2000). Remnants of a Cretaceous intra-oceanic subduction system within the Yarlung-Zangbo suture (southern Tibet). Earth and Planetary Science Letters, 183, 231-244. DOI: 10.1016/S0012-821X(00)00287-9

Aitchison. J. C. and Davis A. M., Evidence for the multiphase nature of the India-Asia collision from the Yarlung Tsangpo suture zone, Tibet Geological Society, London, Special Publications, 226, 217-233, 1 January 2004, https://doi.org/10.1144/GSL.SP.2004.226.01.12

Argus, D. F., Gordon, R. G., and DeMets, C. (2011), Geologically current motion of 56 plates relative to the no-net-rotation reference frame, Geochem. Geophys. Geosyst., 12, Q11001, doi:10.1029/2011GC003751.

Bardintzeff. J. M. & Liégeois, J.-P & Bonin, Bernard & Bellon, Hervé & Rasamimanana, Georges. (2010). Madagascar volcanic provinces linked to the Gondwana break-up: Geochemical and isotopic evidences for contrasting mantle sources. Gondwana Research. 18. 295-314. 10.1016/j.gr.2009.11.010.

Baxter A.T., Aitchison J.C., Ali J.R., Chan J.S.L., Heung Ngai Chan G., Detrital chrome spinel evidence for a Neotethyan intra-oceanic island arc collision with India in the Paleocene, Journal of Asian Earth Sciences, Volume 128, 2016, Pages 90-104, ISSN 1367-9120, https://doi.org/10.1016/j.jseaes.2016.06.023.

Bouilhol P., Jagoutz O., Hanchar J. M., Dudas O. F., Dating the India– Eurasia collision through arc magmatic records, Earth and Planetary Science Letters,

Volume 366, 2013, Pages 163-175, ISSN 0012-821X, https://doi.org/10.1016/j.epsl.2013.01.023.

Buckman S. , Aitchison J.C., Nutman A.P., Bennett V.C., Saktura W. M., Walsh M.J.J, Kachovich S., Hidaka H., The Spongtang Massif in Ladakh, NW Himalaya: An Early Cretaceous record of spontaneous, intra-oceanic subduction initiation in the Neotethys, Gondwana Research, Volume 63, 2018, Pages 226-249, ISSN 1342-937X, https://doi.org/10.1016/j.gr.2018.07.003.

Cande S.C., Patriat P., Dyment J., Motion between the Indian, Antarctic and African plates in the early Cenozoic, Geophysical Journal International, Volume 183, Issue 1, October 2010, Pages 127–149, https://doi.org/10.1111/j.1365-246X.2010.04737.x

Cande. S. & Stegman. D. (2011). Indian and African Plate motions driven by the push force of the Reunion plume head. Nature. 475. 47-52. 10.1038/nature10174.

Chenet A. L., Courtillot V., Fluteau F., Gérard M., Quidelleur X., Khadri S. F. R., Subbarao K. V., Thordarson T. 2009 Determination of rapid Deccan eruptions across the Cretaceous–Tertiary boundary using paleomagnetic secular variation: 2. Constraints from analysis of eight new sections and synthesis for a 3500-m-thick composite section; Journal of Geophysical Research 114/38. doi: 10.1029/2008JB005644

Chenet A. L., Fluteau F., Courtillot V., Gerard M., Subbarao K.V. 2008 Determination of rapid eruption across the Cretaceous–Tertiary boundary using paleomagnetic secular variation: Results from a 1200 m thick section in the Mahabaleshwar escarpment; Journal of Geophysical Research 113 (B4), B04101.

Clennett, E. J., Sigloch, K., Mihalynuk, M. G., Seton, M., Henderson, M. A., Hosseini, K., et al. (2020). A quantitative tomotectonic plate reconstruction of western North America and the eastern Pacific basin. Geochemistry, Geophysics, Geosystems, 21, e2020GC009117. https://doi.org/10.1029/2020GC009117

DeMets C, Merkouriev S, Detailed reconstructions of India–Somalia Plate motion, 60 Ma to present: implications for Somalia Plate absolute motion and India–Eurasia Plate motion, Geophysical Journal International, Volume 227, Issue 3, December 2021, Pages 1730–1767, https://doi.org/10.1093/gji/ggab295

Dessai A.G., Griffin W.L., Decratonization and reactivation of the southern Indian shield: An integrated perspective, Earth-Science Reviews, Volume 220, 2021, 103702, ISSN 0012-8252, https://doi.org/10.1016/j.earscirev.2021.103702.

Di-Cheng Zhu, Sun-Lin Chung, Xuan-Xue Mo, Zhi-Dan Zhao, Yaoling Niu, Biao Song, Yue-Heng Yang; The 132 Ma Comei-Bunbury large igneous province: Remnants identified in present-day southeastern Tibet and southwestern Australia. Geology 2009;; 37 (7): 583–586. Doi: https://doi.org/10.1130/G30001A.1

Dyment J., Evolution of the Carlsberg Ridge between 60 and 45 Ma: Ridge propagation spreading asymmetry and the Deccan-Reunion hotspot, Journal of Geophysical Research, vol. 103, no. B10, pages 24,067-24,084, October 10, 1998

Eagles G., Hoang Ha H., Cretaceous to present kinematics of the Indian, African and Seychelles plates, Geophysical Journal International, Volume 196, Issue 1, January 2014, Pages 1–14, https://doi.org/10.1093/gji/ggt372

Eagles G., Wibisono A. D., Ridge push, mantle plumes and the speed of the Indian plate, Geophysical Journal International, Volume 194, Issue 2, August 2013, Pages 670–677, https://doi.org/10.1093/gji/ggt162

Forsyth D., Uyeda S., On the Relative Importance of the Driving Forces of Plate Motion, Geophysical Journal International, Volume 43, Issue 1, October 1975, Pages 163–200, https://doi.org/10.1111/j.1365-246X.1975.tb00631.x

Georgen J. E., Lin J., Dick H. J. B., Evidence from gravity anomalies for interactions of the Marion and Bouvet hotspots with the Southwest Indian Ridge: effects of transform offsets, Earth and Planetary Science Letters, Volume 187, Issues 3–4, 2001, Pages 283-300, ISSN 0012-821X, https://doi.org/10.1016/S0012-821X(01)00293-X.

Ghatak A, Basu A. R., Vestiges of the Kerguelen plume in the Sylhet Traps, Northeastern India, Earth and Planetary Science Letters, Volume 308, Issues 1–2, 2011, Pages 52-64, ISSN 0012-821X, https://doi.org/10.1016/j.epsl.2011.05.023.

Gibbons A.D., Zahirovic S., Müller R.D., Whittaker J.M., Yatheesh V., A tectonic model reconciling evidence for the collisions between India, Eurasia and intra-oceanic arcs of the central-eastern Tethys, Gondwana Research, Volume 28, Issue 2, 2015, Pages 451-492, ISSN 1342-937X, https://doi.org/10.1016/j.gr.2015.01.001.

Gibbons, A. D., Whittaker, J. M., and Müller, R. D. (2013), The breakup of East Gondwana: Assimilating constraints from Cretaceous ocean basins around India into a best-fit tectonic model, J. Geophys. Res. Solid Earth, 118, 808–822, doi:10.1002/jgrb.50079.

Granot, R., Dyment, J. & Gallet, Y. Geomagnetic field variability during the Cretaceous Normal Superchron. Nature Geosci 5, 220–223 (2012). https://doi.org/10.1038/ngeo1404

Griffin W.L., A.F. Kobussen, E.V.S., Babu S.K., O'Reilly S. Y., Norris R., Sengupta P., A translithospheric suture in the vanished 1-Ga lithospheric root of South India: Evidence from contrasting lithosphere sections in the Dharwar Craton, Lithos, Volume 112, Supplement 2, 2009, Pages 1109-1119, ISSN 0024-4937, https://doi.org/10.1016/j.lithos.2009.05.015.

Gurnis M., Torsvik T. H.; Rapid drift of large continents during the late Precambrian and Paleozoic: Paleomagnetic constraints and dynamic models. Geology 1999; 22 (11): 1023–1026. Doi: https://doi.org/10.1130/00917613(1994)022<1023:RDOLCD>2.3.CO;2

Hafkenscheid, E., Wortel, M. J. R., and Spakman, W. (2006), Subduction history of the Tethyan region derived from seismic tomography and tectonic reconstructions, J. Geophys. Res., 111, B08401, doi:10.1029/2005JB003791.https://doi.org/10.31223/X5CS5N

Ingle S., Weis D., Scoates J. S., Frey F. A., Relationship between the early Kerguelen plume and continental flood basalts of the paleo-Eastern Gondwanan margins, Earth and Planetary Science Letters, Volume 197, Issues 1–2, 2002, Pages 35-50, ISSN 0012-821X, https://doi.org/10.1016/S0012-821X(02)00473-9.

J.G. Ogg, Chapter 5 – Geomagnetic Polarity Time Scale, Editor(s): Felix M. Gradstein, James G. Ogg, Mark D. Schmitz, Gabi M. Ogg, Geologic Time Scale 2020, Elsevier, 2020, Pages 159-192, ISBN 9780128243602, https://doi.org/10.1016/B978-0-12-824360-2.00005-X.

Jagoutz, O., Royden, L., Holt, A. et al. Anomalously fast convergence of India and Eurasia caused by double subduction. Nature Geosci 8, 475–478 (2015). https://doi.org/10.1038/ngeo2418

Jaupart C., Mareschal J. C., The thermal structure and thickness of continental roots, Lithos, Volume 48, Issues 1–4, 1999, Pages 93-114, ISSN 0024-4937, https://doi.org/10.1016/S0024-4937(99)00023-7.

Jay A. E. and Widdowson M. 2008 Stratigraphy, structure and volcanology of the south-easts Deccan continental flood basalt province: implications for eruptive extent and volumes; Journal of the Geological Society London 165, 177-188.

Kale, V.S. (2020). Cretaceous Volcanism in Peninsular India: Rajmahal–Sylhet and Deccan Traps. In: Gupta, N., Tandon, S. (eds) Geodynamics of the Indian Plate. Springer Geology. Springer, Cham. https://doi.org/10.1007/978-3-030-15989-4_8

Keller G., Nagori M. L, Chaudhary M, Reddy N.A., Jaiprakash B.C., Spangenberg Jorge E., Mateo P., Adatte T., Cenomanian-Turonian sea-level transgression and OAE2 deposition in the Western Narmada Basin, India, Gondwana Research, Volume 94, 2021, Pages 73-86, ISSN 1342-937X, https://doi.org/10.1016/j.gr.2021.02.013.

Kumar, P., Yuan, X., Kumar, M. et al. The rapid drift of the Indian tectonic plate. Nature 449, 894–897 (2007). https://doi.org/10.1038/nature06214

Kumari V., Tandon S.K., Kumar N., Ghatak A., Epicontinental Permian-Cretaceous seaways in central India: The debate for the Narmada versus Godavari rifts for the Cretaceous-Tertiary incursion, Earth-Science Reviews, Volume 211, 2020, 103284, ISSN 0012-8252, https://doi.org/10.1016/j.earscirev.2020.103284.

Lonsdale, P. (1983), Overlapping rift zones at the 5.5°S offset of the East Pacific Rise, J. Geophys. Res., 88(B11), 9393– 9406, doi:10.1029/JB088iB11p09393.

Malinverno, A., Quigley, K. W., Staro, A., & Dyment, J. (2020). A Late Cretaceous-Eocene geomagnetic polarity timescale (MQSD20) that steadies spreading rates on multiple mid-ocean ridge flanks. Journal of Geophysical Research: Solid Earth, 125, e2020JB020034. https://doi.org/10.1029/2020JB020034

Morgan, J.P. and Parmentier, E.M. (1984), Lithospheric stress near a ridge-transform intersection. Geophys. Res. Lett., 11: 113-116. https://doi.org/10.1029/GL011i002p00113

O'Neill C., Müller D., Steinberger B., Geodynamic implications of moving Indian Ocean hotspots, Earth and Planetary Science Letters, Volume 215, Issues 1–2, 2003, Pages 151-168, ISSN 0012-821X, https://doi.org/10.1016/S0012-821X(03)00368-6.

Olierook H. K. H, Jourdan F., Merle R. E., Timms N. E, Kusznir N., Muhling J. R., Bunbury Basalt: Gondwana breakup products or earliest vestiges of the Kerguelen mantle plume? Earth and Planetary Science Letters, Volume 440, 2016, Pages 20-32, ISSN 0012-821X, https://doi.org/10.1016/j.epsl.2016.02.008.

Parsons A. J., Hosseini K., Palin R. M., Sigloch K., Geological, geophysical and plate kinematic constraints for models of the India-Asia collision and the post-Triassic central Tethys oceans, Earth-Science Reviews, Volume 208, 2020, 103084, ISSN 0012-8252, https://doi.org/10.1016/j.earscirev.2020.103084.

Patriat, P., Achache, J. India–Eurasia collision chronology has implications for crustal shortening and driving mechanism of plates. Nature 311, 615–621 (1984). https://doi.org/10.1038/311615a0

Pick, T., Tauxe, L. Geomagnetic palaeointensities during the Cretaceous normal superchron measured using submarine basaltic glass. Nature 366, 238–242 (1993). https://doi.org/10.1038/366238a0

Plummer, P.S. (1996), The Amirante ridge/trough complex: response to rotational transform rift/drift between Seychelles and Madagascar. Terra Nova, 8: 34-47. https://doi.org/10.1111/j.1365-3121.1996.tb00723.x

Poornachandra Rao G. V. S., Mallikharjuna Rao J., Palaeomagnetism of the Rajmahal Traps of India: Implication to the Reversal in the Cretaceous Normal Superchron, Journal of geomagnetism and geoelectricity, 1996, Volume 48, Issue 7, Pages 993-1000, Released on J-STAGE May 25, 2007, Online ISSN 2185-5765, Print ISSN 0022-1392, https://doi.org/10.5636/jgg.48.993,

Pusok A. E. and Stegman D. R. 2020 The convergence history of India-Eurasia records multiple subduction dynamics processes; Science Advances 6, eaaz8681.

Rodriguez M., Arnould M., Coltice N., Soret M., Long-term evolution of a plume-induced subduction in the Neotethys realm, Earth and Planetary Science Letters,

Sangode S. J., Dongre A., Bhagat A. R., Meshram D., Discovery of Deccan

Inclination anomaly and its possible geodynamic implications over the Indian Plate (Article in Press: Journal of Earth System Sciences).

Schaeffer A. J., Lebedev S., Global shear speed structure of the upper mantle and transition zone, Geophysical Journal International, Volume 194, Issue 1, July 2013, Pages 417–449, https://doi.org/10.1093/gji/ggt095

Stoddard, P. R., and Abbott, D. (1996), Influence of the tectosphere upon plate motion, J. Geophys. Res., 101(B3), 5425– 5433, doi:10.1029/95JB03540.

Storey, B. The role of mantle plumes in continental breakup: case histories from Gondwanaland. Nature 377, 301–308 (1995). https://doi.org/10.1038/377301 a0

Talukdar, S.C., Murthy, M.V.N. The Indian traps, their tectonic history, and their bearing on problems of Indian flood basalt provinces. Bull Volcanol 35, 602–618 (1971). https://doi.org/10.1007/BF02596831

Torsvik T.H, Tucker R.D, Ashwal L.D, Eide E.A, Rakotosolofo N.A, de Wit M.J, Late Cretaceous magmatism in Madagascar: palaeomagnetic evidence for a stationary Marion hotspot, Earth and Planetary Science Letters, Volume 164, Issues 1–2, 1998, Pages 221-232, ISSN 0012-821X, https://doi.org/10.1016/S0 012-821X(98)00206-4.

Van der Meer D.G., van Hinsbergen D. J. J., Spakman W., Atlas of the nderworld: Slab remnants in the mantle, their sinking history, and a new outlook on lower mantle viscosity, Tectonophysics, Volume 723, 2018, Pages 309-448, ISSN 0040-1951, https://doi.org/10.1016/j.tecto.2017.10.004.

Van Hinsbergen, D. J. J. (2019). Comment on "Comparing paleomagnetic study means with apparent wander paths: A case study and paleomagnetic test of the Greater India versus Greater Indian Basin hypotheses" by David B. Rowley. Tectonics, 38, 4516– 4520. https://doi.org/10.1029/2019TC005525

Van Hinsbergen, D. J. J., Steinberger, B., Doubrovine, P. V., and Gassmöller, R. (2011), Acceleration and deceleration of India-Asia convergence since the Cretaceous: Roles of mantle plumes and continental collision, J. Geophys. Res., 116, B06101, https://doi:10.1029/2010JB008051.

Van Hinsbergen, D.J.J., Steinberger, B., Guilmette, C. et al. A record of plume-induced plate rotation triggering subduction initiation. Nat. Geosci. 14, 626–630 (2021). https://doi.org/10.1038/s41561-021-00780-7

Vandamme D., Courtillot V., Besse J., Montigny R. 1991 Palaeomagnetism and age determinations of the Deccan Traps (India); results of a Nagpur– Bombay traverse and review of earlier work; Reviews of Geophysics 29, 159–190.Volume 561,2021, 116798, ISSN 0012-821X, https://doi.org/10.1016/j.epsl.2021.116798

White L.T., Lister G.S., The collision of India with Asia, Journal of Geodynamics, Volumes 56–57, 2012, Pages 7-17, ISSN 0264-3707, https://doi.org/10.101 6/j.jog.2011.06.006.

Zahirovic S., Müller R. D., Seton M., Flament N., Tectonic speed limits from plate kinematic reconstructions, Earth and Planetary Science Letters, Volume 418, 2015, Pages 40-52, ISSN 0012-821X, https://doi.org/10.1016/j.epsl.2015.02.037.

Zahirovic, S., Müller, R. D., Seton, M., Flament, N., Gurnis, M., and Whittaker, J. (2012), Insights on the kinematics of the India-Eurasia collision from global geodynamic models, Geochem. Geophys. Geosyst., 13, Q04W11, doi:10.1029/2011GC003883.

Table 1: Data table showing the results obtained after statistical treatment of paleomagnetic data.

	Chron 30n.y D I	C29r.y D I	C29n.y D I			
Central Tendency						
Window Mean after applying the Filter.	-366	-56	-193 (333.3 antipode)	-65	-377	-50
Scatter	-95: 2.5; k = 21.37, N:153	-95: 1.1, k = 36.05, N: 451	-95: 4.3, k:21.61, N: 54			
Anomaly with Vandamme *et al.* 1991	+4 (clockwise)	(shallow)	(anticlockwise)	+5 (deeper)	+0.8 (clockwise)	(shallow)
Anomaly with Réunion latitudes*		$+1^0$		$+10^0$		^{0}

Table 2. Calculated drift rates from the inclination data for Central tendency and filtered mean data respectively for GTS2020 and MQSD2020 timescales.

	Central Tendency (Latitudinal drift)	Filtered Mean (Latitudinal drift)	Central Tendency (Longitudinal drift)	Filtered Mean (Longitudinal drift)	Central Tendency (Diagonal drift)	Filtered Mean (Diagonal drift)
Distance covered in degrees	0	0	0	0	0	0
Distance covered in kilometres	km	km	km	km	km	km
Spreading rate (GTS 2020)	mm yr^{-1}	mm yr^{-1}	mm yr^{-1}	mm yr^{-1}	mm yr^{-1}	mm yr^{-1}
Spreading rate (MQSD20)	mm yr^{-1}	mm yr^{-1}	mm yr^{-1}	mm yr^{-1}	mm yr^{-1}	mm yr^{-1}

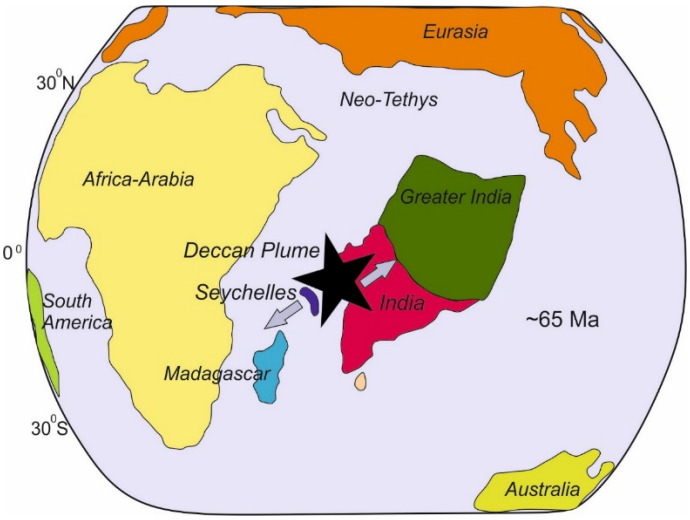

Fig 1. Position of the Indian subcontinent during the Deccan Trap Volcanism during 65 Ma (redrawn after Van Hinsbergen et al 2011).

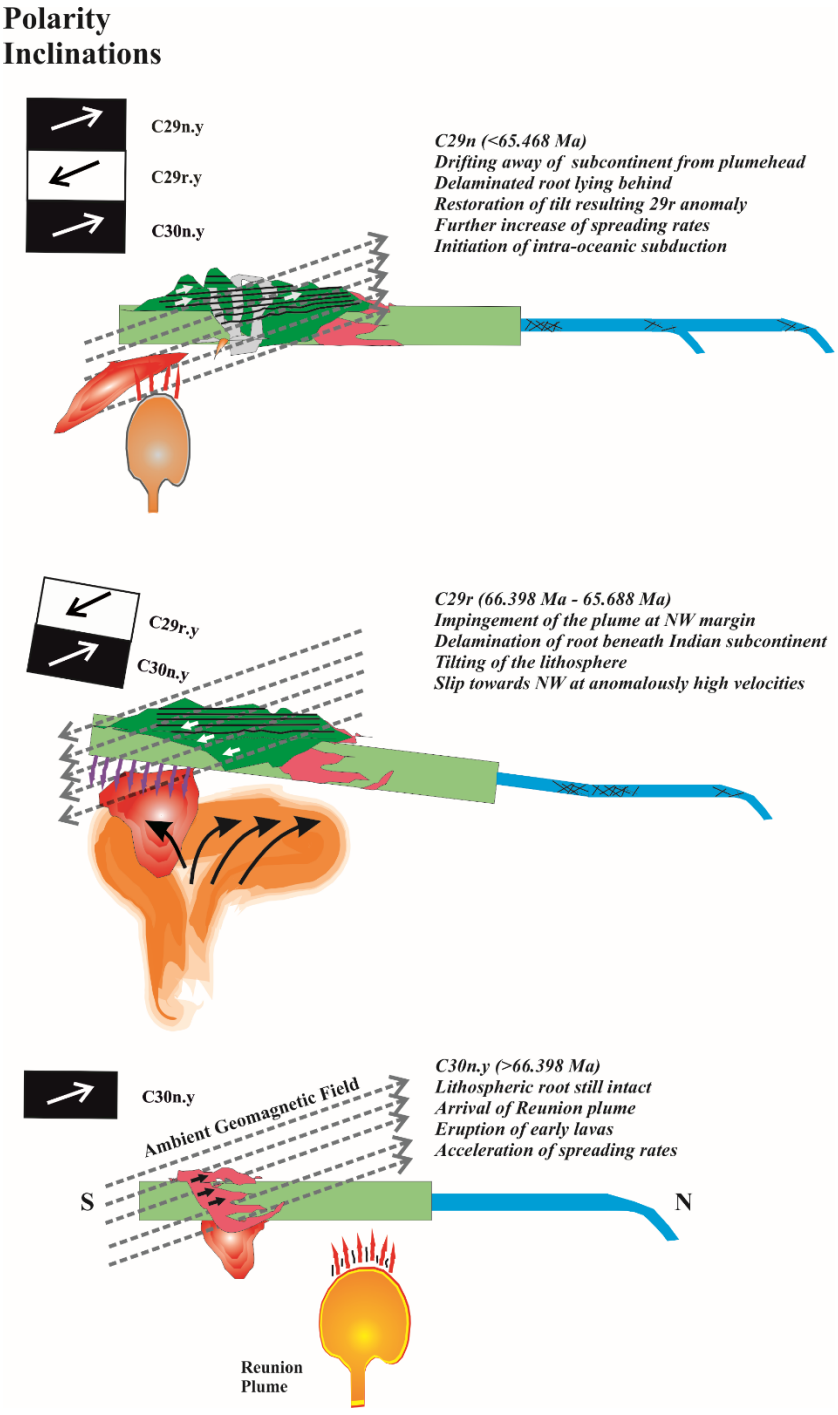

Fig 2. The mechanism of Deccan inclination anomaly modified after

Sangode et al 2022. At C30n the plume-head arrives beneath the Indian subcontinent resulting in minor alkaline intrusives. This is followed by the main phase of eruption at C29r which led to tilting of the Indian subcontinent towards north by ~10°, along with the delamination of the lithospheric root below the subcontinent. The root delamination led to an increase in buoyancy, further contributing to the anomalous drift rates and slip towards NW. At C30n during, the subcontinent moved away from the plume-head, restoring normal inclination values along the northeastwardly march of Indian subcontinent.

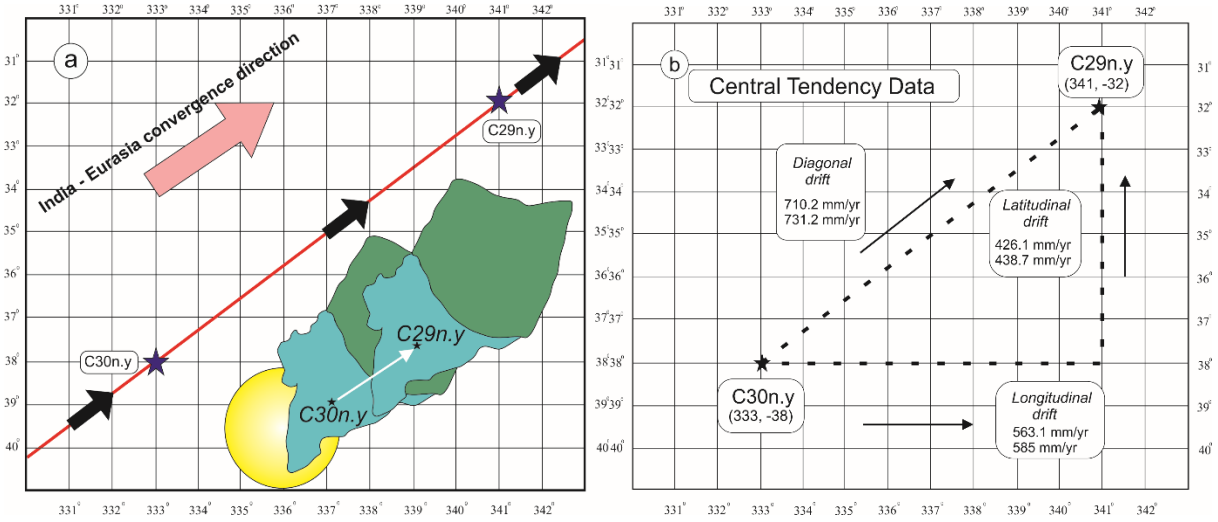

Fig 3. Model A: North-eastward drift of the Indian subcontinent can be observed along with the calculated drift rates based on inclination data. a)The blue stars indicate initial and final positions for the Indian subcontinent during the chrons C30n.y and C29n.y. The black arrows point the directions of drift calculated from the present study. The larger grey arrow indicates the established convergence direction of Indian subcontinent with respect to Eurasia, while the red line marks the trace of the drift direction as deduced from the paleomagnetic data. The yellow circle represents Reunion plume, blue portion indicates the present day extent of Indian subcontinent and the green portion indicates subducted continental part of Greater India. The small black stars represent the position of present day city of Nagpur in central India, which was used as a reference point to conduct the calculations. The small white arrow depicts the relative motion of the subcontinent at initial and final positions, showing the northeastward drift of India. b) The black stars mark the initial and final positions of the Indian subcontinent. Longitudial (563.1 and 585 mmyr^{-1}), latitudinal (426.1 and 438.7 mmyr^{-1}), and the diagonal

(710.2 and 731.2 mmyr^{-1}) drift rates have been calculated by extrapolating the vectors from initial and final positions along respective directions. Two different spreading rates result from using the dates for chrons C30n.y and C29n.y for MQSD20 and GTS 2020, where the above mentioned period spans 1.518 and 1.563 Ma respectively, resulting higher drift rates for MQSD20 and slightly lower rates for GTS2020.

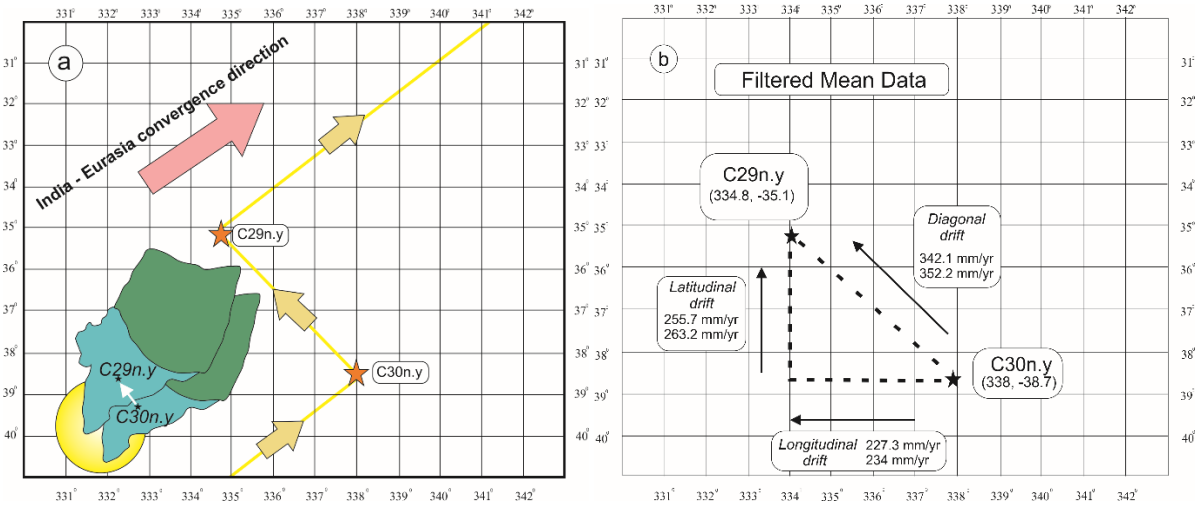

Fig 4. Model B: North-westward drift of the Indian subcontinent can be observed along with the calculated drift rates based on inclination data. *a)* The orange stars indicate initial and final positions for the Indian subcontinent during the chrons C30n.y and C29n.y. The smaller arrows point the direction of drift calculated from the present study. The larger grey arrow indicates the established convergence direction of Indian subcontinent with respect to Eurasia, while the yellow line marks the trace of the drift direction as deduced from the paleomagnetic data. The yellow circle represents the Reunion plume, blue portion indicates the present day extent of Indian subcontinent while the green portion indicates subducted continental Greater India. The small black stars represent the position of present day city of Nagpur in central India, which was used as a reference point to conduct the calculations. The small white arrow depicts the relative motion of the subcontinent at initial and final positions. It can obeserved clearly that the northeastward motion of India was interrupted when it encountered the Reunion plume at ~65Ma leading to a change of convergence direction at anomalously high velocities. The model thus predicts that the plume push emanating from the Reunion plume did overcome the slab pull and ridge push forces acting on the Indian plate during its encounter for a short period of time. This change in direction was corrected once the Indian subcon-

tinent moved away from the sphere of direct influence of the Reunion plume. *b)* The black stars mark the initial and final positions of the Indian subcontinent. Longitudial (227.3 and 234 mmyr^{-1}), latitudinal (255.7 and 263.2 mmyr^{-1}), and diagonal (342.1 and 352.2 mmyr^{-1}) drift rates have been calculated by extrapolating the vectors from initial and final positions along respective directions. Two different spreading rates result from using the dates for chrons C30n.y and C29n.y for MQSD20 and GTS 2020, where the above mentioned period spans 1.518 and 1.563 Ma respectively, resulting higher drift rates for MQSD20 and slightly lower rates for GTS2020.

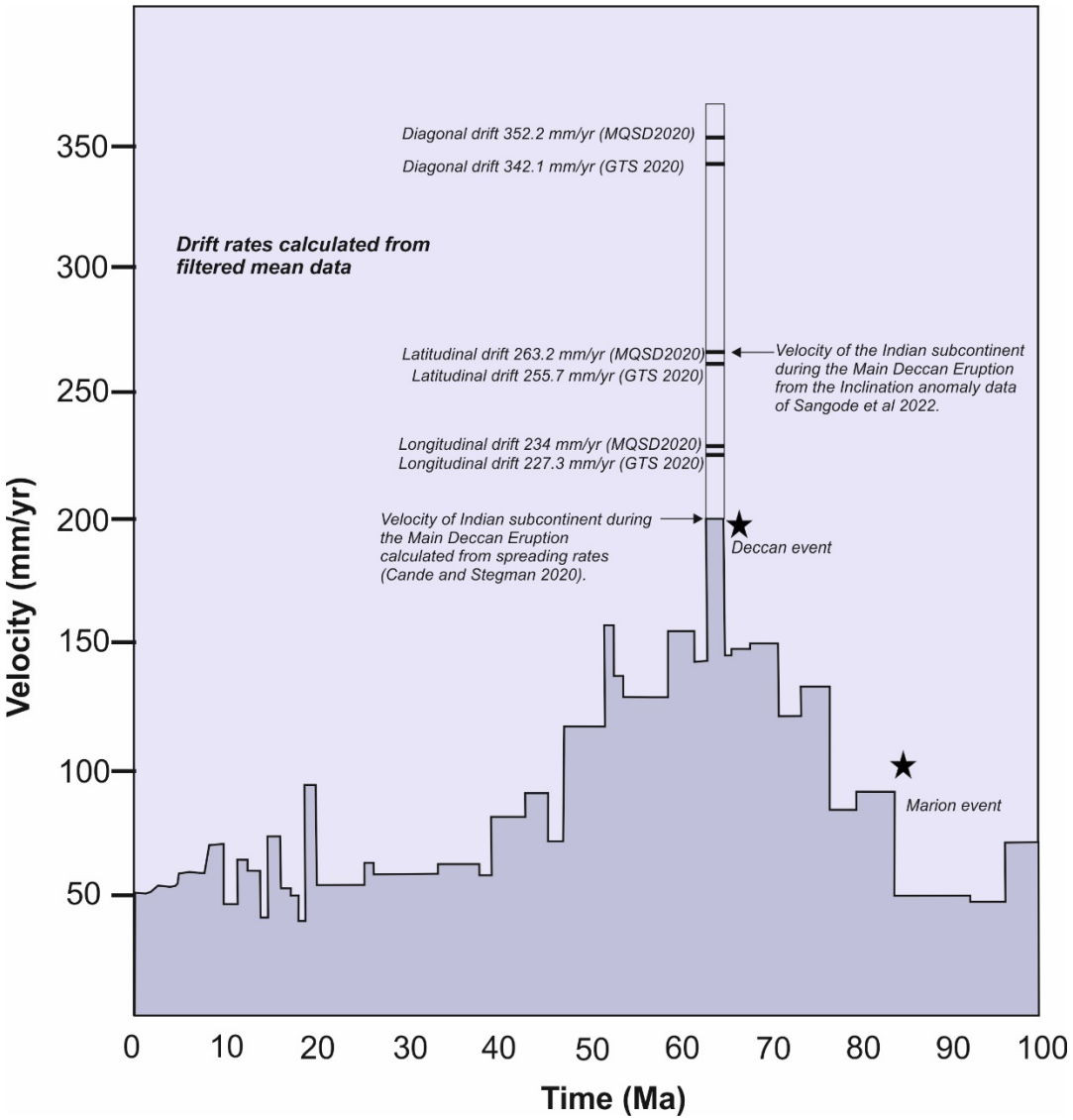

Fig 5. A plot showing spreading rates versus time of the Indian plate for the past 100 Ma, modified after White and Lister (2012). At the Deccan event, the new data has been plotted to depict the newly discovered drift rates from the filtered mean data for the Indian Subcontinent. The black stars mark mantle plume events. The drift rates for the Indian subcontinent peak at the Deccan event, following which there is a considerable decrease in drift rates. This has been attributed to the moving away of the subcontinent from the Reunion hotspot leading to increasing viscosity of the asthenosphere beneath the Indian subcontinent acting as an obstruction to the rapid drift.

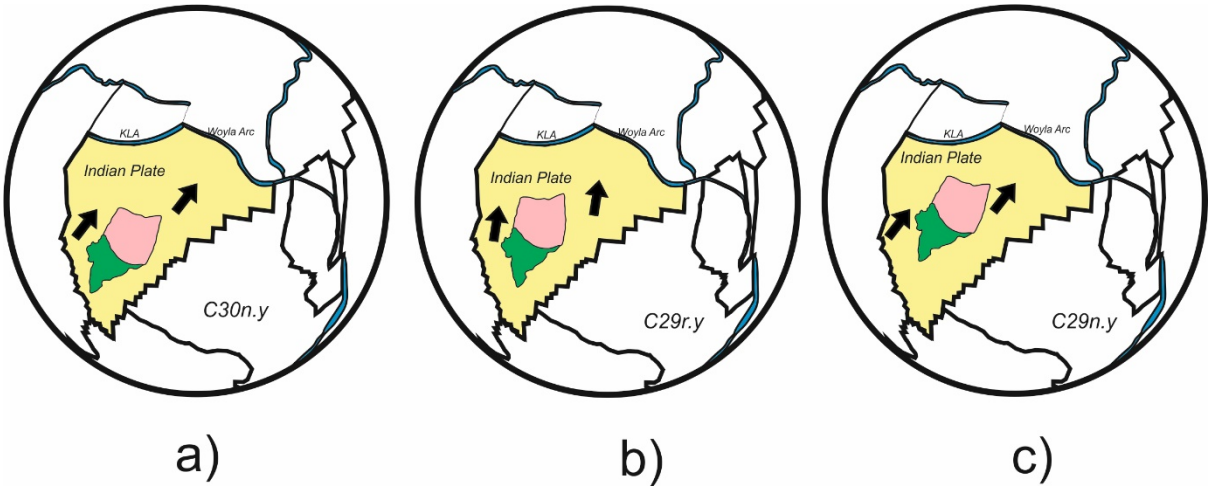

Fig 6. Arrangement of the plate boundaries for Indian plate at time of interaction with the Reunion plume (after Gibbons et al 2015). The convergence directions for C29r depicting a slight change for the Indian subcontinent which was restored substantially back to normal after the Deccan event.

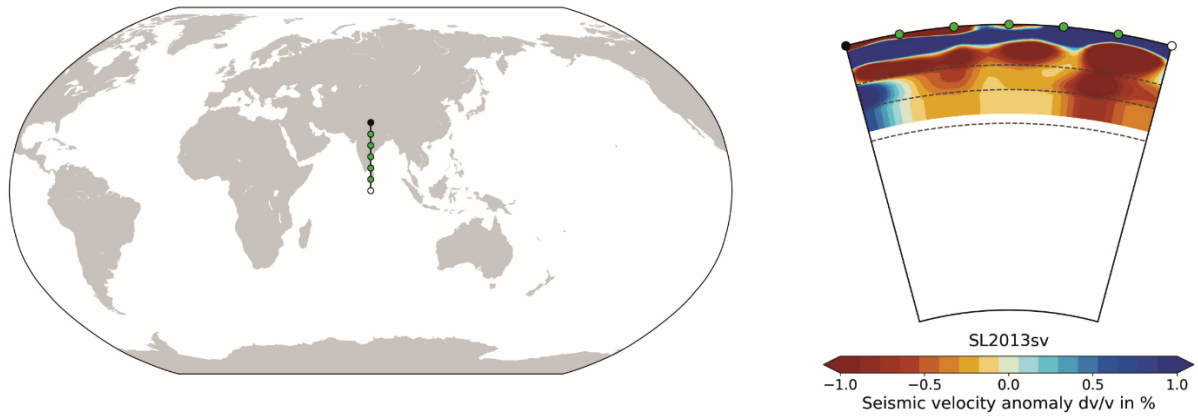

Fig 7. A seismic tomographic cross section of the upper mantle from the model SL2013sv (Schaeffer and Lebedev, 2013) for the present-day Indian subcontinent along 80°E from 30°N to 0°, showing absence of any high-density material below the Indian subcontinent hinting towards the absence of a cratonic root, which if present would have impeded the plate velocities.

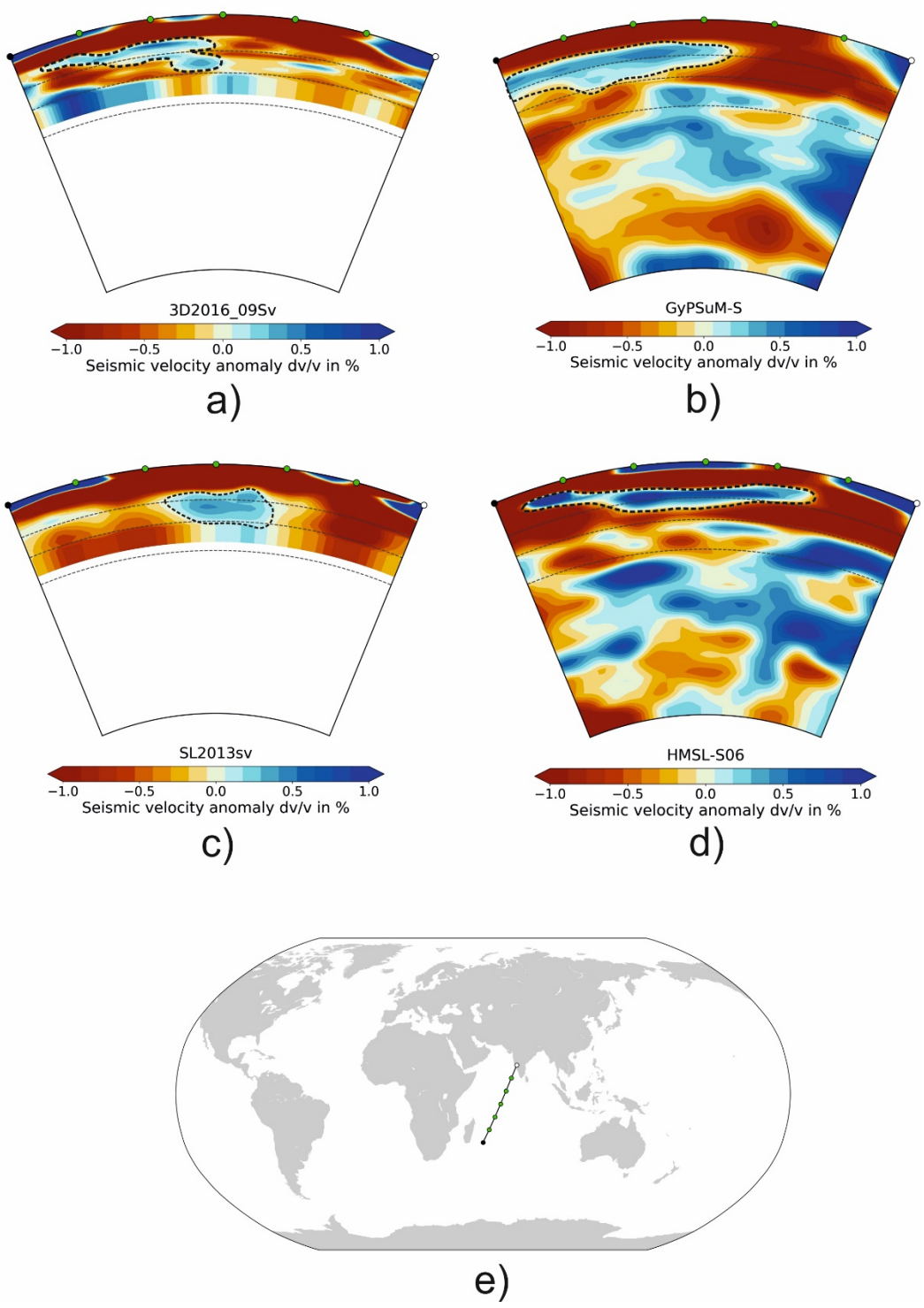
3D2016_09Sv
−1.0 −0.5 0.0 0.5 1.0
Seismic velocity anomaly dv/v in %
a)
GyPSuM-S
−1.0 −0.5 0.0 0.5 1.0
Seismic velocity anomaly dv/v in %
b)
SL2013sv
−1.0 −0.5 0.0 0.5 1.0
Seismic velocity anomaly dv/v in %
c)
HMSL-S06
−1.0 −0.5 0.0 0.5 1.0
Seismic velocity anomaly dv/v in %
d)
e)

Fig 8. Seismic tomographic s-wave profiles for the mantle. Cross sections from (25°S, 55°E) and (15°N, 75°E) based on (3D2016_09Sv), (GyPSuM-S), (HMSL-S06) and (SL2013sv), depicting the proposed lithospheric root/keel dislodged from the Indian subcontinent during the Deccan episode.

This manuscript bearing reference Number- JESS-D-21- 00662R2 has been accepted for publication in the Journal of Earth System Sciences (Published by the Indian Academy of Sciences) and can be considered In Press.

Palaeomagnetic Inclination Anomaly in the Deccan traps and its geodynamic implications over the Indian Plate

S. J. Sangode*, Ashish Dongre, Amarjeet Bhagat and Dhananjay Meshram

Department of Geology, Savitribai Phule Pune University, Pune (India) 411 007

* Corresponding Author e-mail: sangode@rediffmail.com

Abstract

Rapid northward drift of the Indian plate during Deccan volcanism assumes a gradual equatorward shallowing of the paleomagnetic inclinations amongst subsequently younger lava flows. Compilation of palaeomagnetic database and using 1062 statistically significant site mean directions from the Deccan Volcanic Province discovered an inclination anomaly of +10 degrees during the Deccan main phase eruptions (DE_M within Chron C29r at 66.398 Ma to 65.688 Ma). This anomaly represents northward tilt during C29r followed by its restoration by C29n (~65 Ma). This anomaly is explained here by the Indian lithospheric response to Réunion plume head during DE_M. A sequence of coincident geodynamic instances including: i) biostratigraphically constrained 'the brief inland seaway', ii) development of a regional southward dips for the lava flows, iii) major drop in sea level at the southern tip of Peninsula and iv) accelerated spreading and convergence rates during C29r to 29n transitions; substantiate the effect of lithospheric tilt and its restoration. We present a plume-lithospheric evolutionary model to explain the anomaly and its wider implications over the Indian lithospheric plate.

Keywords: Deccan traps; Palaeomagnetism; Indian plate; Réunion hotspot; Late Cretaceous

1 Introduction

Recent studies on mantle plume-lithosphere interactions have indicated that the spreading plume heads below lithosphere can develop significant asthenospheric flows to exert 'plume-push' force and act as potential drivers for accelerated plate motions and/or subduction initiation (e.g., Cande and Stegman 2011; van Hinsbergen *et al.* 2011; Pusok and Stegman 2020). The Deccan Large Igneous Province (LIP) is a product of such lithospheric interactions with Réunion hotspot during the northwardly drift of the Indian plate in the Late Cretaceous and early Paleogene (Courtillot *et al.* 1986; Basu *et al.* 1993). LIPs are characterized by short-lived (<1-5 Ma) igneous pulses responsible for large volume (>75%) magma outpourings (Bryan and Ernst 2007). Geochronological records indicate a peak in tholeiitic basalt eruptions of Deccan volcanism during 66.4-65.4 Ma (Sprain *et al.* 2019 and references therein), precisely within the geomagnetic Chron C29r. This peak is widely referred to as the Main Deccan eruption phase (denoted here as DE_M) representing the bulk Deccan volcanism (~80%, Renne *et al.* 2015; Schoene *et al.* 2015; Sprain *et al.* 2019) which is also evident from abundance of palaeomagnetic reversal records of C29r (e.g., Vandamme et al. 1991; Chenet et al., 2009).

Several aspects on Deccan volcanism largely dealt with stratigraphy, petrology, structures and morphology; and the geodynamic implications of Réunion mantle plume over Indian lithospheric plate is inadequately explored (e.g. Raval and Veeraswamy 2019). The rapid northward drift of the Indian plate, along with its rotation, during Deccan encounter, has been previously studied by many workers (Cande and Stegman 2011; van Hinsbergen et al 2011; Pusok and Stegman 2020) using various computational models. Extensive palaeomagnetic data has been produced from Deccan basalts since 50s representing the classical geomagnetic polarity sequence of C30n-29r-29n (e.g., Clegg *et al.* 1955; Wensink 1973; Vandamme *et al.* 1991; Chenet *et al.* 2008; 2009). In this study, we have examined the palaeomagnetic data by compilation of over 1600 significant site mean palaeomagnetic directions from over 76 published records from Deccan trap (Fig. 1 and Supplementary data file) for its possible geodynamic implication.

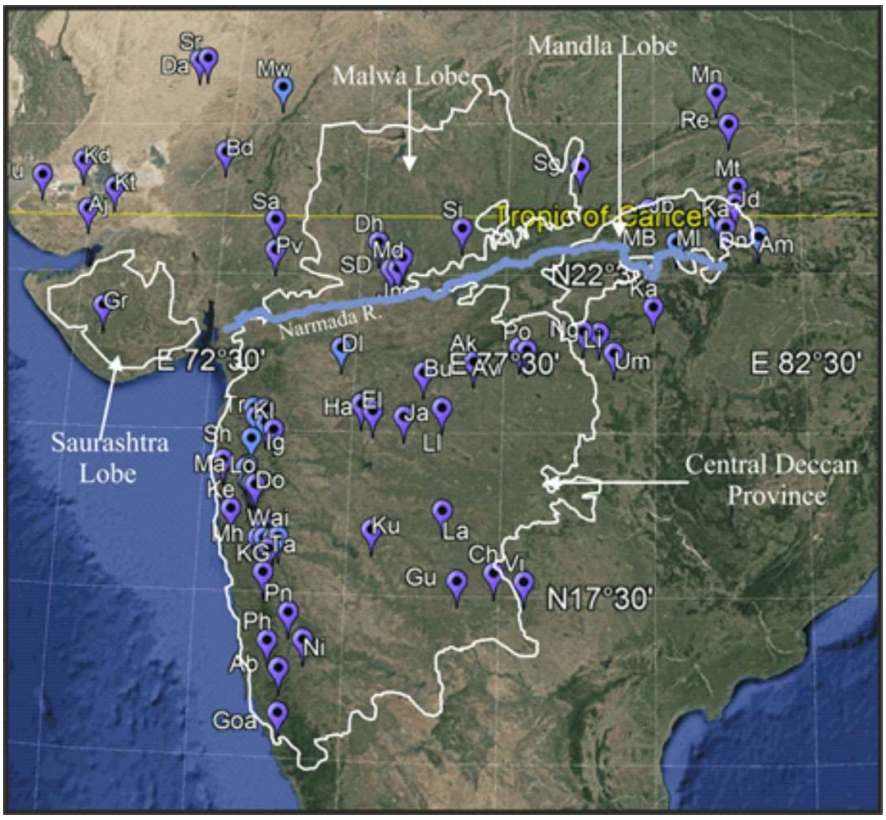

Figure 1: Map showing present-day extent of the Deccan traps into four distinct sub-provinces (Malwa, Mandla, Saurashtra and Central Province). The dots with abbreviations (expanded below) are the sites where paleomagnetic studies were undertaken by previous workers and taken into consideration for present analysis (details in SDF Table D6). The sub-provinces north of the Narmada/Tapi rifts (i.e., Malwa, Mandla and Saurashtra) dominantly exhibit the records of earliest eruptions belonging to Chron C30n as a result of northward drift of the Indian plate after its breakup from Gondwana. In the northern region of the central province, majority of the normal polarity flows overlay the reverse polarity, and rest of the occurrences with prominent reverse polarity (C29r) compile the tripartite subdivision of the Deccan traps into the C30n-C29r-C29n sequence. Stratigraphically thicker (/longer) records of C29r are most widely documented in the Central province. *Site Abbreviations*- Amboli (Ab) , Anjar (Aj), Akola (Ak), Ambenali (Al), Amarkantak (Am), Amravati (Av), Badargarh (Bd), Buldhana (Bu), Chincholi (Ch), Dandali (Da), Dhar (Dh), Dhule (Dl), Dindori (Dn), Dongargarh (Do), Ellora (El), Goa (Goa), Girnar (Gr), Gulbarga (Gu), Harsul (Ha), Igatpuri (Ig), Jalna (Ja), Jabalpur (Jb), Jodhpur (Jd), Jamdarwaza (Jm), Jumara (Ju), Karopani (Ka), Khairi (Ka), Kalodungar (Kd), Kelgar (Ke), Khumbharli Ghat (KG), Khandala (Kh), Kalsubai (Kl) , Khodala (Ko), Khopoli (Kp), Kanthkote (Kt), Kurduwadi (Ku), Latur (La), Linga (Li), Lonar lake (Ll), Lonavala (Lo), Matheran (Ma), Mandla Bridge (MB), Mandaleshwar (Md), Mahabaleshwar (Mh), Mandla (Ml), Manikpur (Mn), Mokhada (Mo), Mohtara (Mt), Mumbai (Mu), Mundwara (Mw), Neral (Ne), Nagpur (Ng), Nipani (Ni), Panchigani (Pa), Phonda (Ph), Panhala (Pn), Pohor (Po), Pavagadh (Pv), Rewa (Re), Rajahmundry (Rj)Sadara

(Sa), Sahastra Dhara (SD), Sagar (Sg), Shahapur (Sh), Singarchori(Si), Sarnu (Sr), Tapola (Ta), Trimbak (Tr), Umred (Um), Varandha Ghat (VG), Vikarabad (Vi), Wai (Wai).

Finally, a compilation based on 56 widely referred publications (See Supplementary data file) with details on analytical treatments and statistical operations was selected for the present analysis. After compilation, the data was classified into the geomagnetic Chrons: C30n, C29r and C29n for further processing. Details on methods, treatment, classification and filtering of the data is discussed below and given in Supplementary data file (SDF). As mentioned, the Chron 29r (66.398 Ma – 65.688 Ma) represents highest number of data points in agreement with the abundance as a result of bulk of lava eruption during D_{EM} (e.g. Vandamme *et al.* 1991; Chenet *et al.* 2008; 2009; Renne *et al.* 2015; Schoene *et al.* 2015; Sprain *et al.* 2019). This robust compilation observed an unambiguous inclination anomaly of more than 10º and clockwise/anticlockwise rotations of 2 to 5 degrees during C29r (see Tables 1 and 2). Aim of this work is therefore to report this inclination anomaly and explain its possible geodynamic implications over the Indian plate.

2 Methodology

The work was initiated by preparation of database by complete documentation of the palaeomagnetic data published since 1955. Over 76 publications including thesis presenting the palaeomagnetic studies from Deccan traps (and dykes) till date were reviewed and the data base presented in excel file format for the processing. The vast majority of these publications unambiguously reported the palaeomagnetic directions (Declinations and Inclinations or D/I) in agreement with the N-R-N sequence of the C30n-29r-29n geomagnetic polarity time scale. The data was independently produced by various teams during over last 65 years, and majority of the analysis performed in reputed national/international laboratories with standard instrumental setups (information given in SDF). We elaborate below the criteria and methods adopted to compile and treat this data with a discussion on the sources of error justifying the anomaly.

The high ferrimagnetic concentration within Deccan basalt mineralogy offers distinct demagnetization spectra measurable with moderate magnetometer sensitivity, and helps easy discrimination of Characteristic remanence (ChRM) components considered as primary remanence.

Majority of the published papers presented the demagnetization data (using thermal and/or alternating fields methods), identification of ChRM directions and the site mean calculations using routine statistical methods with spherical distribution (e.g., Fisher 1967, 1987). The parameters of statistical significance (e.g., alpha-95, precision parameter and maximum angular deviations) describe the scatter, facilitating filtering of the data for higher reliability and quality (McElhinny 1964; Fisher 1967, 1987; Tarling 1983). In majority of cases, the reverse polarity is unambiguously assigned to C29r, the reversal followed by normal to C29r-29n, and the normal followed by reversal to 30n-29r polarity chrons. The data was supported by field stratigraphic knowledge, chemostratigraphy and the isotope geochronology wherever available, by these authors (list of references given in SDF).

For present analysis, we complied only the declination/inclination (D/I) values from the published data, facilitating the site mean data points (See SDF). This is because, the NRM intensities can show large variation due to the style of presentation, various laboratory standards and instrumental sensitivities from individual attempts (discussed in SDF). The palaeomagnetic analysis involve various protocols of demagnetization adopted by different workers and instrumental sensitivities (Collinson, 1983; Tarling 1983; Butler 1992; McElhinny et al 2000; Tauxe 2010; Dunlop and Ozdemir 1997). Therefore, the standardization and comparison of NRM intensities across different attempts is not feasible. However, since our inferences are founded entirely on the D/I data, the NRM intensities are therefore neglected.

2.1 *Sources of Error*

The data were retrieved and rechecked several times avoiding typographic errors. Further below, we discuss the sources of errors based on which the filtering strategy was adopted.

1) Manual error: The first and foremost source of error is generally developed during the collection of oriented samples in the field. The oriented samples are collected manually (oriented hand samples) or by gasoline-driven portable rock coring machines (manually handled). The samples are marked carefully using either the compass north or by the sun compass. This has a greater chance of introducing manual errors at various stages from marking

in the field till creating the standard cylindrical specimens in laboratory. Manual errors can also be introduced during laboratory handling of the specimens for analysis, as for most of the spinner magnetometers, the specimens are to be handled over six directions of measurement strategy. There is no clue to define the manual error, although it may be reflected in the final data as scatter and can be refined by the statistical distribution or calculation of means from large number of specimens. We find majority of the data is not tilt corrected, since the tilt is regional and non-measurable at outcrop level unless mapped (e.g., See Chenet et al 2009 p. 5 mention). This has encouraged to record the physical tilt of the palaeomagnetic data as discovered in this work.

2) Laboratory standards: The palaeomagnetic data in Deccan traps are produced from various laboratories that are commonly equipped with spinner magnetometers. High NRM intensities amongst Deccan trap basalts often permit pronounced demagnetization paths, even with low sensitivity magnetometers (e.g., Minispin from Molspin UK, Sensitivity: 0.05 mA/m). The other commonly used spinner magnetometers with better sensitivities are DSM-Schonstedt (~10e-4 A/m) and JR- 4 to 6 versions of AGICO Czech (~2.4 x μA/m). Both of these later versions provided better details of demagnetization trajectories over a large number of palaeomagnetic specimen. Whereas, the quality of older data which was meticulously produced from other instruments such as Astatic magnetometers, is also ascertained by excellent repeatability over stronger intensities of the Deccan basalt samples. Recently, the fully automated magnetometers AGICO (JR 6A) prevented manual errors from sample positioning; and the standardized data interface software with statistical and plotting provisions allowed rapid, error-free data processing. The cryogenic magnetometer (e.g., 2G) gives the finest sensitivity in paleomagnetic analysis; however, the strong remanence in Deccan basalt does not compel such analysis unless the studies like paleointensity and secular variation are intended.

The detailed palaeomagnetic analysis involve demagnetization of a large array of specimens to produce statistically significant data by the removal of noisy results (Collinson 1965; Butler 1992; Tarling 1983; Tauxe 2010). The two most commonly used methods of demagnetization are thermal and alternating field (af) demagnetizations. While thermal demagnetization can introduce laboratory-induced errors during heating and cooling, alternating field (af) demagnetization is the most commonly used in Deccan traps due to majority of soft ferrimagnetic- primary and secondary components (Vandamme et al., 1991). Individual workers have used different protocols of demagnetization strategy, and the demagnetizers themselves can introduce spurious fields during analyses, producing deviations rather than direct errors. Furthermore, the skills and experience of individual workers during interpretation varies, which may lead to some manual bias error component.

3) Geomagnetic variability and transitional fields: Some authors have indicated secular variation or the non-dipole fields as the source of error in paleomagnetic directions acquired by few samples. However, such samples showing spurious directions are most likely to be rejected, as the palaeomagnetic directions for Deccan traps are very well known and constrained. Similar is the case for the transitional polarity instances that are developed during normal to reversal or vice versa producing intermediate and mixed polarities. These directions are also likely to be rejected by individual authors, and if they are present in the data, the filtering criteria used in this paper has taken care for removal of such intermediate and noisy directions.

4) Geotectonics: The shield type geometry of Deccan province in general refutes any major intra-shield tectonics to significantly affect the palaeomagnetic directions. No major internal rotations and deformation have so far been reported within palaeomagnetic data from the Deccan province. Chron C29r is the main focus of this study, and majority of the palaeomagnetic data for this chron belong to the main/central Deccan province, which does not show such intra-shield tectonic deformations to significantly influence the palaeomagnetic

data. Nevertheless, if such incoherence is present, it will be reflected by the internal deviations of D/I values, and our filtering criteria (discussed below) has taken care.

2.2 *Data Reduction (rejection) and Filtering*

The Deccan traps represent one of the richest databases over a short geological time interval of less than 5 Ma, and is marked by the distinct polarity sequence of N-R-N for the Late Cretaceous/Paleogene. The ample data thus produced from the Deccan traps, from various laboratories therefore is in close agreement. Previously, Vandamme *et al.* (1991) produced Deccan Super pole based on the compilation of the available data. With the updated database (till 2020), we further recalculated the Deccan Super pole, which is in close agreement with Vandamme *et al*. (1991) (see Table 1) depicting a central tendency. Therefore, a simple filtering and reduction criteria was used based on the qualitative parameters (Alpha-95, k and MAD) derived from the routine statistical methods in palaeomagnetism (Tauxe 2010). The deviation of values seen in this table (Table 1) is mainly due to enrichment from new data points added during the latter 30 years (1062 points in this study against the 163 points of Vandamme et al., 1991). Therefore, considering these Super pole directions as central tendency, we further defined the limits/windows for filtering of the data in this work given in Table 2. The data was classified into the chrons C30n, C29r and C29n and then the central tendency (Table 1) was used to filter the data by a declination window of $+/-36^0$ (i.e., 10% of 360^0) and inclination window of $+/-18^0$ (i.e., 10% of 180^0) and is presented in Table 2.

Table 1: An account of the mean paleomagnetic data recalculated from the database presented in Supplemental data file (SDF).

	Total data points	**Mean D/I**	**Super-pole**	**Mean Inclination Data**		
				C30n	**C29r**	**C29n**
Vandamme *et al*. (1991)	163	154/43 (antipode: 334/-43)	281˚E 37˚N	D/I ----	D/I 154/44	D/I 333/-48
This Study	1062	152/56 (antipode: 332/-56)	284˚E 27˚N	333/-38	157/47	341/-32

Table 2: Considering the means for whole data in 5th to 6th columns of Table 1 as the central tendency for the updated database (SDF), we further applied filters to remove the noise in mean data due to the possible errors described in the text. The data for C30n, C29r and C29n are filtered individually in a declination window of +/- 36 (10% of 360) and inclination window of +/-18 (10% of 180).

	Chron 30n		**C29r**		**C29n**	
	D	**I**	**D**	**I**	**D**	**I**
Central Tendency	333	-38	157	47	341	-32
Window	297-366	20-56	121-193	29-65	305-377	14-50
Mean after applying the Filter.	338	-38.7	153.3 (333.3 antipode)	47.4	334.8	-35.1
Scatter	α-95: 2.5; k = 21.37, N:153		α -95: 1.1, k = 36.05, N: 451		α -95: 4.3, k:21.61, N: 54	
Anomaly with Vandamme *et al.* 1991	+4 (clockwise)	-5 (shallow)	-0.7 (anti-clockwise)	+5 (deeper)	+0.8 (clockwise)	-8 (shallow)
Anomaly with Réunion latitudes*		$+1^0$		$+10^0$		-2^0

Note: α-95: 'size of the cone in degrees within which the true palaeomagnetic direction is expected to lie with 95% confidence'; k: 'measure of the concentration of the distribution about the true mean direction', N: number of samples/sites/stratigraphic time horizon. *: Considering the Reunion latitude of 21^0, the inclination of ~37.5^0 can be derived using Geocentric axial dipole model reference frame of Torsvik et al (2012), calculated using IAPD 2014 Software.

3 The Inclination Anomaly and Rotation

It can be noted from the table 2, that the observed mean inclination for C29r is significantly higher than the anticipated paleolatitude derivative of 37º at Reunion latitudes. This inclination anomaly of the order of 10^0 is further attested by various approaches given in Table 3.

Table 3: The Inclination Anomaly for C29r with respect to 30n and 29n, using various approaches described in text and table 2. The mean of central tendency after filtering for C29r is taken as 47^0.

Reference	**Inclination in degrees**	**C29r Anomaly Amount in Degree**
w.r.t. Expected latitudes using *Tan I = 2 Tanλ* (*λ = 20.5 to 21.5 for Reunion)*	~36 to 38	11 to 9
w.r.t. C30n from Table 1	38	9
w.r.t. C29n from Table 1	32	15
w.r.t. C30n Filtered Mean (Table 2)	38.7	8.7
w.r.t. C29n Filtered Mean (Table 2)	35.1	12.3
w.r.t. Reunion latitude mean	37	10.4
Average anomaly from various approaches		$10.78^0 \sim +11^0$ or $+10^0$

Finally, we consider this inclination anomaly of '+11º' or broadly '+10º' as mathematical expression for significant northerly/northeasterly dip achieved by the Indian plate during C29r. Further its restoration is evident from the negligible anomaly near the expected inclination for the chron C29n. The C29r anomaly is therefore much oversighted in the context of equatorward drift of the Indian plate, which anticipated either inclination shallowing or the inclination values intermediate between C30n and C29n within the Deccan sequence. Moreover, no evidence for such large magnitude changes during the Late Cretaceous geodynamo exists (Coe *et al.* 2000; Pechersky *et al.* 2010; Velasco-Villareal *et al.* 2011), and therefore refutes such anomalous geodynamo behaviour related explanations. In contrast, coincident geological evidences from the Indian subcontinent endorse the anomaly by possible effect of plate tilting (described later).

Similar to inclination anomaly, the declination data finds anomalies (See Table 4) depicting 5º clockwise rotation during C29r with respect to C30n and 2º anticlockwise rotation in C29n with respect to C29r. Based on this palaeomagnetic information, we present a cartoon model (fig. 2) to depict the geodynamic interaction of the Indian lithospheric plate with Réunion plume head, and in order to explain the evidences of anomaly in the text.

Table 4: Rotational anomaly (+: clockwise, -: anticlockwise) derived from the central tendency and filtered data (depicted in tables 1-3).

Chron	Filtered Mean	Wrt Reference North	Inferred Indian plate rotation
C29n	334.8	-25.2	2 degree anticlockwise w.r.t. 29r
C29r	333.3	-26.7	5 degree clockwise w.r.t. 30n
C30n	338	-22	
During 80 to 60 Ma		-12	

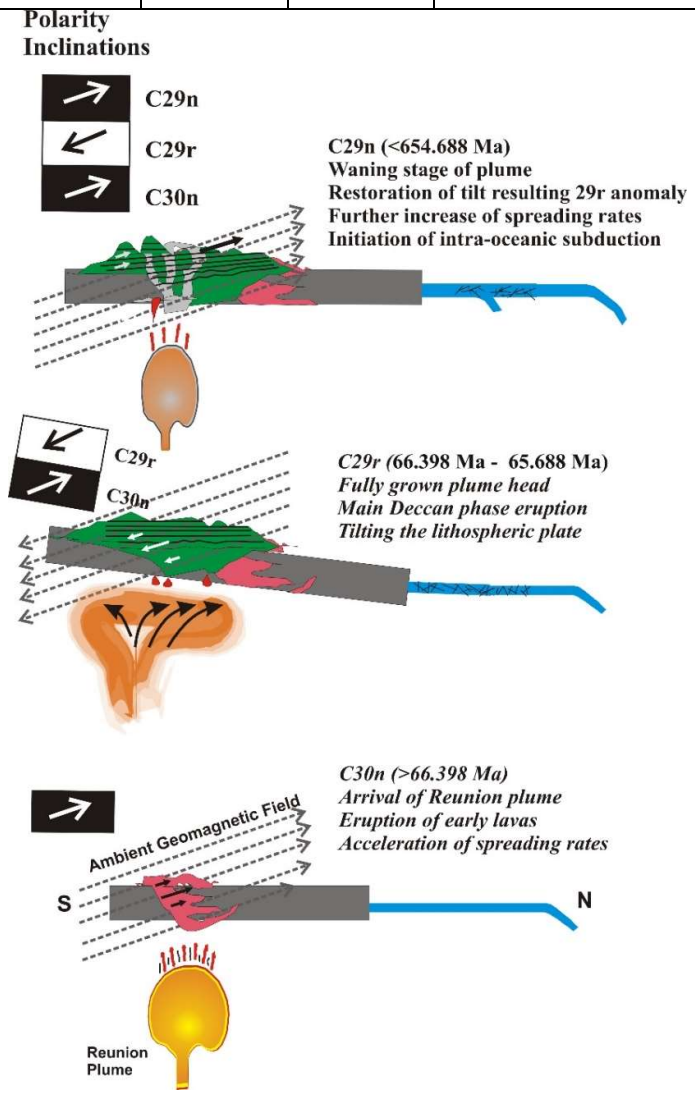

Figure 2. Cartoon model showing Reunion plume head-lithospheric interaction for Indian plate during Deccan eruption. The model depicts geodynamic mechanism to impart the inclination anomaly

as described in text. During C30n, the subcontinent approached the impinging mantle plume, and is recorded by alkaline magmatism in the northern Deccan province. The plate interaction with fully developed plume head during C29r resulted in north/northeast tilt. As the plate moved farther from the waning plume, the tilt was restored, and reverse inclination steepened, producing the inclination anomaly of C29r.

4 Geodynamic Implications

Considering the tilt and rotation estimates based on palaeomagnetic data (Tables 1 to 4 and SDF); the cartoon model (Fig. 2) explains the possible geodynamic mechanism with implications to Reunion plume-lithospheric interactions. This follows the coincident geological evidences from the published records discussed below.

Very high inclinations (D/I=140/60º) during C29r were reported from the Deccan traps in southern latitudes of Deccan province (Mishra *et al.* 1989). Although the data is inadequate and the precise chronology not available; it suggests an existence of southern/ plate wide extent of the tilt. The pre-Deccan, Late Cretaceous strata from Cauvery Basin in the southern Peninsula record a shallower inclination (338/-38, N=80) (Venkateswarulu 2020), further substantiate existence of Deccan anomaly relative to the pre- Deccan strata. Whereas, the inclinations for C29n and C30n agrees well with the anticipated paleolatitudes (Table 3), which indicates that the tilt was absent in C30n and restored during C29n as the Indian plate drifted away from the Réunion plume head (e.g., see Fig. 2). The regional southward dip for the Deccan lava flows (Fig. 3c and d) is widely documented (Jay and Widdowson 2008; Shoene *et al.* 2015) that verify the proposed model (Fig. 2) based on the palaeomagnetic information.

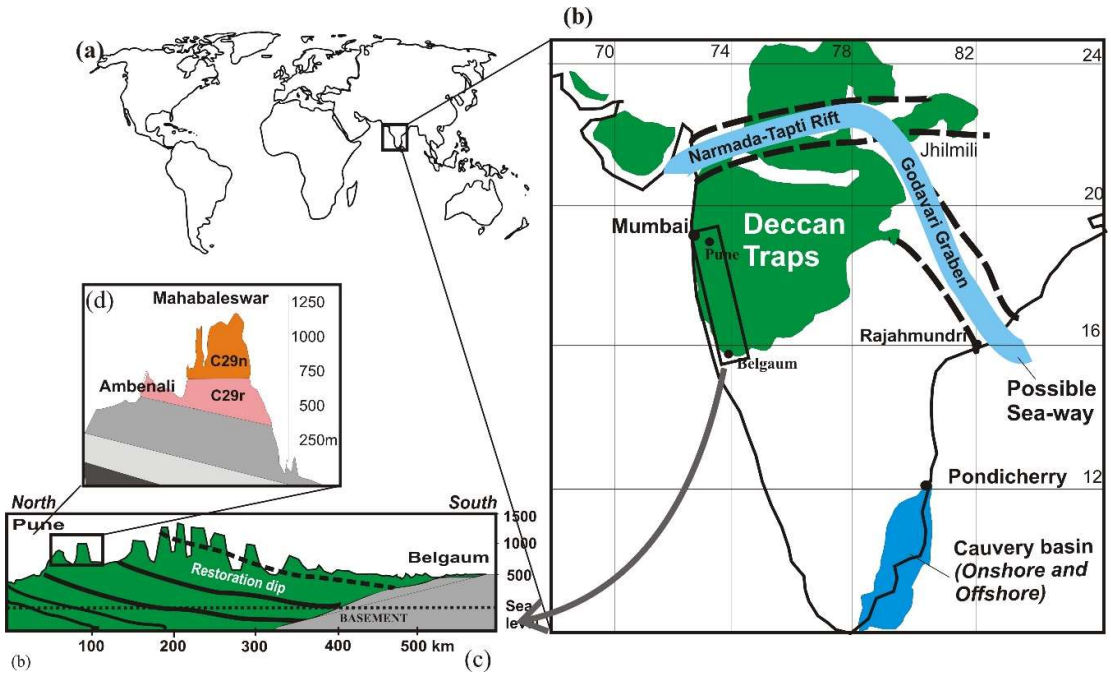

Figure 3. (a) World map showing the location of Deccan Province, (b) Part of Indian plate marking the present extent of Deccan trap province and the possible seaway as reported from biostratigraphic records discussed in text. The broad location of Cauvery Basin is shown which documented significant drop in sea level during the Late Cretaceous. The widely reported Pune to Belgaum (N-S) profile (c) depict a regional southward dip, explained here as a result of tilt restoration (discussed in text). Inset (d) shows the dip discordance between C29r (Ambenali Formation) and C29n (Mahabaleswar Formation) marked by Schoene *et al.* (2021), as evidence of tilt and its restoration.

4.1 *Magmatic records of plume head arrival and the Plate tilt*

There is close temporal and spatial linkage between voluminous LIPs, their tholeiitic and alkaline magmatism and mantle plumes (e.g., Bryan and Ernst 2007). LIPs are typically characterized by large volume (>75%) magma outpourings within very short time interval (<1-5 Ma, Bryan and Ernst 2007). The relatively rapid drift of the Indian plate did not permit its longer exposure to the Reunion plume. Whereas the highly effusive and voluminous outpouring of magma suggest a buoyant lithospheric interaction, and hence a significant geodynamic response of the Indian plate during Deccan volcanism is anticipated.

Alkaline rocks associated with LIPs are typically formed due to low degree of partial melting owing to minor thermal effects from an impinging or receding mantle plume (e.g., Gibson *et al.* 2006).

The impact of Réunion plume over Indian plate is in close agreement with this convention through the observed episodes of tholeiitic and alkaline magmatism. The initial impact of the Réunion plume head started ~0.2 million years before the DE_M and produced nepheline syenites and alkali gabbros during these early Deccan eruptions (Fig. 3). This corresponds to terminal C30n and early C29r stage. Recent high-precision geochronological data (Renne *et al.* 2015; Sprain *et al.* 2019) indicated outpouring of bulk Deccan tholeiites between 65.4 and 66.4 Ma within C29r. This rapid extrusion requires higher amounts of partial melting under a considerably elevated geothermal gradient during a fully developed plume head, which precisely coincides with the duration of C29r (Cande and Kent 1995). Small-volume, volatile-rich magmatism of lamprophyres and carbonatites between 65.8-65.2 Ma (Fig. 3), which were mostly emplaced towards the terminal part of the $DE_{M,}$ typically intruded the Deccan lavas. This terminal phase is an artifact of small-fraction melting caused by thermal weakening during the waning stage of the Réunion plume. The occurrence of DE_M precisely within C29r therefore elucidates the short span of geodynamic interaction of the plume head with the Indian plate. The rapid impact of plume head below the western margin of the Indian plate therefore appears to have resulted in a major geodynamic activity as recorded by the tilt and rotation in the paleomagnetic data inferred here.

Further, the lithospheric tilt and its restoration had been physically recorded by the flows showing a southerly tilt. Apart from other widely reported field evidences for the regional dip (e.g., Jay and Widdowson 2008), recently Schoene *et al.* (2021) reported discordance between C29n and 29r flows (reproduced in Fig. 3d) that indicate the restoration of tilt during C29n. It is also likely that the restoration may not be complete and the residual tilt is reflected in the southeasterly flows of the major Peninsular rivers (except Narmada which flows in rift). The questions remain unsolved in this context of the relative adjustments of Malwa plateau with Central Deccan province separated by the Narmada rift. So detailed investigations are also necessary to estimate a possible component of sea level rise in the southern stratigraphy during tilt restoration. Investigations are also needed to find the relationships amongst post- buoyant subsidence, rotation and relative sea level changes.

4.2 *Accelerated convergence at the end of C29r*

Sea floor spreading anomalies document accelerated spreading rates in the Indian Ocean reaching a maximum between ~66 and 63 Ma during C29n (Cande and Stegman 2011; compiled and redrawn in Fig. 4). The initial anomalously high rates of drift of the Indian plate from less than 100 mm/y to ~160 mm/y during 68 to ~66 Ma were explained by the arrival of the plume head (Eagles and Hoang 2014). However, the later increase in the drift (up to 180 mm/y after ~66 Ma) during the waning and withdrawal stages of the plume/plume head remains little explored. We suggest the later increase due to convergence as a result of a combination of different factors including *i)* the termination of resistance from plume-induced rotational and tilt components to the northward drifting kinematics, *ii)* the establishment of double subduction (explained below) in front of Indian plate easing out the northward drift of the Indo-Australian plate. This demands a detailed estimates using kinematic modeling to elaborate the above contentions arising out of the Deccan tilt, and is beyond the scope of the present work.

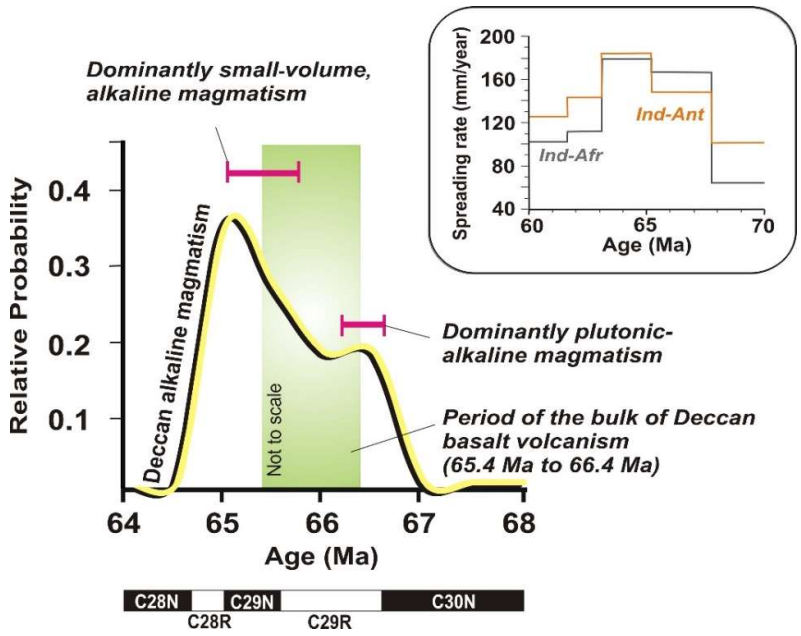

Figure 4. Relative probability of alkaline and small-volume, volatile rich magmatism spatially and temporally related to the Deccan LIP based on high-precision $^{40}Ar/^{39}Ar$ and U-Pb determinations (n=12) (adopted from Dongre, *et al.* 2021). The period of bulk Deccan basalt volcanism is also shown in green

(from Sprain *et al.*, 2019). *Inset*: Spreading rates between India-Antarctica and India-Africa ridges (After Cande and Stegman, 2011).

4.3 *Acceleration of the intra-oceanic subduction*

Mantle plumes have been considered as drivers of regional subduction initiation (Gerya *et al.* 2015; Pusok and Stegman 2020; van Hinsbergen *et al.* 2021, Rodriguez *et al.* 2021). Multiple and the double subductions are evident for the India-Asia convergence (See Hafkenscheid *et al* 2006; Bouilhol *et al* 2013; Replumaz *et al* 2014; Jagoutz *et al* 2015 and 2019;; Searle 2019; Rodriguez *et al* 2021). The final subduction around ~66 Ma to 65 Ma is little explored in the context of Deccan volcanism and the Réunion plume push force. We infer that the quick geodynamic response of the Indian plate to Réunion plume head during DE_M marked by the tilt and counter (clockwise/anticlockwise) rotations during C29r might have exerted significant changes in the pre-existing plate kinematics at the India-Asia subduction interface. The possible resultant deformation due to plate tilt and rotation added to the rapid changes in rates of convergence may have significant repercussions on the colder/brittle/thinner ocean floor in front of the northern Indian continental margin to deform leading to an intra-oceanic subduction (Fig. 2). In absence of any detailed study, therefore we postulate that the Réunion plume lithospheric interaction was significant enough to accelerate the convergence during late subduction.

4.4 *Brief Opening of inland 'Sea-way'*

Based on paleontological finds, a short-lived 'seaway' associated with Deccan traps precisely at the end of C29r has been widely reported (e.g. Keller *et al.* 2009, 2012 and references therein). This inland 'sea-way' formation (/marine influence) along pre-existing rift valleys (i.e. Narmada and Godavari Rifts, shown in Fig. 3) is evident by the stressed marine fauna. The brief north/northeastward tilting of the Indian plate therefore offers a possibility to explain the formation of the brief inland 'sea-way'.

Biostratigraphically, the well-documented localities ~800-1000 km inland of the Narmada and Godavari rifts contain brief and stressed planktic foraminiferal assemblages within terrestrial palustrine to freshwater facies (Keller *et al.* 2009, 2012). The absence of benthic species among these localities (Keller *et al.* 2012) indicates only a brief marine incursion; which can be explained due to the coincident lithospheric tilt and submergence of the rift valley. The contemporary low base levels of Godavari and

Narmada rifts would have facilitated the dramatic relative sea level change in response to the tilt for the reported marine incursions. The paleosols developed immediately over this zone of marine excursion (Keller *et al.* 2012) designate upland conditions by withdrawal of sea and further support the restoration of tilt during C29n (depicted in Fig. 2).

The late Maastrichtian rocks of Cauvery basin at the southern tip of Peninsular India represent fluvial formations overlain by marine to estuarine formations and record a vertical sea level fall of 80 m (Raju *et al.* 1994; Nagendra and Reddy 2017). Thus, upliftment of the southern peninsular tip of the Indian plate is documented and marked by a rapid sea level fall during the deposition of Kallamedu Formation (Late Maastrichtian) in the Cauvery Basin. The 80m fall in sea level reported by Raju et al (2005) is therefore coincident and can be postulated as a result of northward tilt of the Indian plate as it moved over, passing the Reunion plume head to cause northern/NE dip uplifting the southernmost part of the plate. Briefly the plume appears to have buoyantly uplifted this southern part of the Indian plate, while the northern and northeastern part dipped. The contemporaneous upliftment of the southern end of the Indian plate along with downward tilt in northern and northeastern Deccan provinces can therefore be related to the geodynamic causes coincident with the Reunion plume lithospheric interactions discussed above. We finally summarize this sequence of events in table 5 with a note for more detailed studies to test several hypothesis arising out of the explanations of coincident geological instances during/after the tilt reported here. On the other hand, more supporting and conflicting geological signatures are to be gathered to further discuss the anomaly and its implications.

Table 5: A summary of sequence of events presented in this paper.

Time	**Stage**	**Event**
C30n	Plume early stage	Indian plate encountered the Réunion hotspot
Late 30n to Early 29r	Emerging plume-lithosphere interaction	Indian plate encountered the plume over western continental margin and rotated possibly by thermal expansion (and uplift) of the lithosphere in the plume region. Eruption of early lavas and alkaline rocks. Acceleration of spreading rates.
Early to Late 29r	Fully developed plume head	Maximum exposure of the plate to plume, eruption of bulk of Deccan basalts, possible upliftment of the southern Peninsular part of the Indian plate along with tilting in the N/NE part of

		the plate, biostratigraphic evidences of 80m drop in sea level in south and opening of the seaway in N/NE periphery of Deccan. Quick clockwise-anticlockwise rotations along with northward tilt appears to have developed a weak (/fracture) zone possibly leading to the latest subduction in the India-Eurasia zone.
29n		Waning stage of the plume, restoration of tilt, regional south dip of Deccan, closure of seaway, onset of secondary subduction

Conclusion

We report a palaeomagnetic inclination anomaly of the order of 10 degrees during the Chron C29r (66.398 Ma – 65.688 Ma) depicting lithospheric tilt for Indian plate and its restoration during C29n (immediately after ~65.7 Ma). At regional scale geological evidences presented here suggest this anomaly as an artifact of the Indian lithospheric response to Reunion plume during the main phase of Deccan eruption. The widespread geological incidences during the N/NE tilting of the Indian plate, during Late C29r Chron includes: i) short. inland, marine incursion in the northern Deccan province in contrast to the sea level fall in the Southern Peninsula, ii) the regional southward dip of C29r lava flows and iii) the initiation of double subduction at the northern margin of Indian plate. The geodynamic interaction of the Reunion hotspot with Indian lithospheric plate deduced from the long term palaeomagnetic database from Deccan basalts further demands detailed kinematic modelling to establish a relationship amongst the plume push force, Deccan volcanism, Indian ocean spreading and the late Himalayan subduction.

Acknowledgements

We indirectly acknowledge all the authors who produced and published the palaeomagnetic data over the years in Deccan traps cited in this paper. SJS, AND and AB acknowledge Ministry of Earth Sciences for funding through MoES/P.O.(Seismo)/1(353)/2018. All the authors acknowledge Head, Department of Geology SPPU, for support during the pandemic. Critical reviews from six referees improved the manuscript and presentations. Mr Pushkar Nalawade is acknowledged for his help in cartography.

Finally, we thank Dr Jyotisankar Ray and Dr Chalapathi Rao for suggestions and improvements along with efficient editorial handling of the manuscript.

There are no conflict of interests.

Authors Statement

SJS, AB and AND conceptualized and planned the study. AB compiled the data, and with SJS curated the data by processing, corrections and presentation. AND, SJS, AB developed the model and DCM added discussions and guidance. All the authors involved in inputs including concepts, writing, discussion, ideas, interpretations, revisions and the presentation of diagrams and tables.

References

Basu A R, Renne P R, Dasgupta D K, Teichmann F, Poreda R J 1993 Early and Late Alkali Igneous Pulses and a High-3He Plume Origin for the Deccan Flood Basalts; *Science* **261**, 902-906.

Bouilhol P, Jagoutz O, Hanchar, JM, Dudas FO, 2013 Dating the India–Eurasia collision through arc magmatic records; Earth Planet. Sci. Lett. 366, 163–175.

Bryan S and Ernst R 2008 Revised Definition of Large Igneous Province (LIP); *Earth Science Reviews*. doi: 10.1016/j.earscirev.2007.08.00.

Butler, R F 1992 Paleomagnetism: Magnetic Domains to Geologic Terranes; Blackwell. ISBN 0-86542-070-X.

Cande S C and Kent D V 1995 Revised calibration of the geomagnetic polarity timescale for the Late Cretaceous and Cenozoic; *Journal of Geophysical Research* **100**, 6093-6095.

Cande S C and Stegman D R 2011 Indian and African plate motions driven by the push force of the Réunion plume head; *Nature* **475**, 47–52.

Chenet A L, Courtillot V, Fluteau F, Gérard M, Quidelleur X, Khadri S F R, Subbarao K V, Thordarson T 2009 Determination of rapid Deccan eruptions across the Cretaceous–Tertiary boundary using paleomagnetic secular variation: 2. Constraints from analysis of eight new sections and synthesis for a 3500-m-thick composite section; *Journal of Geophysical Research* **114/38**. doi: 10.1029/2008JB005644.

Chenet A L, Fluteau F, Courtillot V, Gerard M, Subbarao KV 2008 Determination of rapid eruption across the Cretaceous–Tertiary boundary using paleomagnetic secular variation: Results from a 1200 m thick section in the Mahabaleshwar escarpment; *Journal of Geophysical Research* 113 (B4), B04101.

Clegg J A, Deutsch E R, Griffiths D H 1956 Rock magnetism in India; *Philos. Mag*. **1**, 419-431.

Coe R S, Hongre L, Glatzmaier G 2000 An examination of simulated geomagnetic reversals from a palaeomagnetic perspective; *Phil. Trans. R. Soc. A*. **358**, 1141–1170 http://doi.org/ 10.1098/rsta.2000.0578(2000)

Collinson D W 1983 Methods in Rock Magnetism and Paleomagnetism; London: Chapman and Hall.

Courtillot V, Besse J, Vandamme D, Montigny R, Jaeger Cappetta H 1986 Deccan flood basalts at the Cretaceous/Tertiary boundary?; *Earth and Planetary Science Letters* **80**, 361-374.

Dongre A, Dhote P S, Zamarkar P, Sangode S J, Belyanin G, Meshram D C, Patil S K, Karmakar A, Jain L 2021 Short-lived alkaline magmatism related to Réunion plume in the Deccan large igneous province: inferences from petrology, 40Ar/39Ar geochronology and paleomagnetism of lamprophyre from the Sarnu-Dandali alkaline igneous complex; *Geological Society London Special Publications* **513**. https://doi.org/10.1144/SP513-2021-34

Dunlop D J and Özdemir Ö. 1997 Rock Magnetism: Fundamentals and Frontiers; Cambridge Univ. Press. ISBN 0-521-32514-5.

Eagles G and Hoang H 2014 Cretaceous to present kinematics on the Indian, African and Seychelles plates; *Geophysical Journal International* **196**, 1-14.

Fisher N I, Lewis T & Embleton B J 1987 Statistical analysis of spherical data; London: Cambridge.

Gerya T V, Stern R J, Baes M, Sobolev S V, Whattam S A 2015 Plate tectonics on the Earth triggered by plume-induced subduction initiation; *Nature* **527**, 221-225, doi:10.1038/nature15752.

Gibson S A, Thompson R N, Day J A 2006 Timescales and mechanisms of plume- lithosphere interactions: 40Ar/39Ar geochronology and geochemistry of alkaline igneous rocks from the Parana-Etendeka large igneous province; *Earth and Planetary Science Letters* **251**, 1-17.

Hafkenscheid E, Wortel M J R, Spakman W, 2006 Subduction history of the Tethyan re-gion derived from seismic tomography and tectonic reconstructions; J. Geophys. Res. 111, B08401.

Jagoutz O, Bouilhol P, Schaltegger U, Müntener O, 2019. The isotopic evolution of the Kohistan Ladakh arc from subduction initiation to continent arc collision. Geol. Soc. Lond., Spec. Publ. 483, 165–182.

Jagoutz, O., Royden, L., Holt, A.F., Becker, T.W., 2015. Anomalously fast convergence of India and Eurasia caused by double subduction. Nat. Geosci. 8, 475–478.

Jay AE and Widdowson M 2008 Stratigraphy, structure and volcanology of the south-easts Deccan continental flood basalt province: implications for eruptive extent and volumes; *Journal of the Geological Society London* **165**, 177-188.

Keller G, Adatte T, Bajpai S, Mohabey DM, Widdowson M, Khosla A, Sharma R, Khosla SC, Gertsch, B, Fleitmann D, Sahni A 2009 K-T transition in Deccan Traps and intertrappean beds in central India mark major marine seaway across India; *Earth and Planetary Science Letters* **282**, 10–23. doi:10.1016/j.epsl.2009.02.016.

Keller G, Adatte T, Bhowmick PK, Upadhyay H, Dave A, Reddy AN, Jaiprakash BC 2012 Nature and timing of extinctions in Cretaceous-Tertiary planktic foraminifera preserved in Deccan intertrappean sediments of the Krishna-Godavari Basin, India; *Earth and Planetary Science Letters* **341–344**, 211–221. doi:10.1016/j.epsl.2012.06.021.

McElhinny, M. W. (1964). Statistical significance of the fold test in paleomagnetism. Goephys. J. Roy. Astron. Soc., 8, pp. 338-340.

McElhinny, Michael W.; McFadden, Phillip L. (2000). Paleomagnetism: Continents and Oceans. Academic Press. ISBN 0-12-483355-1.

Mishra DC, Gupta SB, Venkatarayudu M 1989 Godavari rift and its extension towards the east coast of India; *Earth and Planetary Science Letters* **94**, 344-352.

Nagendra R and Reddy AN 2017 Major geologic events of the Cauvery Basin, India and their correlation with global signatures: A review; *Journal of Palaeogeography* **6(1)**, 69-83.

Pechersky DM, Lyubushin AA, Sharonova ZV 2010 On the synchronism in the events within the core and on the surface of the earth: The changes in the organic world and in the polarity of the geomagnetic field in the phanerozoic; **Physics of the Solid Earth 46**, 613-623.

Pusok AE and Stegman DR 2020 The convergence history of India-Eurasia records multiple subduction dynamics processes; *Science Advances* **6**, eaaz8681.

Raju DSN, Jaiprakash BC, Ravindran CN, Kalyanasunder R, Ramesh P 1994 The magnitude of hiatus and sea level changes across the K T boundary in Cauvery and Krishna Godavari Basin; *Jour. Geol. Soc. India*, **44**, 301-315.

Raval U and Veeraswamy K 2019 Some apparent space-time mismatches (puzzles) over the Indian subcontinent and channeling; *Journal of the geological society of India* **93**, 25-32.

Renne PR, Sprain CJ, Richards MA, Self S, Vanderkluysen L, Pande K 2015 State shift in deccan volcanism at the cretaceous-Paleogene boundary, possibly induced by impact; *Science* **350(6256)**, 76-78.

Replumaz, A., Capitanio, F.A., Guillot, S., Negredo, A.M., Villaseñor, A., 2014. The coupling of Indian subduction and Asian continental tectonics. Gondwana Res. 26, 608–626.

Rodriguez M, Arnould M, Coltice N, Soret M, Hoang E 2021 Long-term evolution of a plume-induced subduction in the Neotethys realm; *Earth and Planetary Science Letters* **561**, 116798. https://doi.org/10.1016/j.epsl.2021.116798

Schoene B, Eddy MP, Keller CB and Samperton KM. 2021 An evaluation of Deccan Traps eruption rates using geochronologic data; *Geochronology* **3**, 181–198

Schoene B, Samperton KM, Eddy MP, Keller G, Adatte T, Bowring S, Khadri SFR, Gertsch B 2015 U-Pb geochronology of the Deccan traps and relation to the end cretaceous mass extinction; *Science* **347**, 182-184.

Searle, M.P., 2019. Timing of subduction initiation, arc formation, ophiolite obduction and India–Asia collision in the Himalaya. Geol. Soc. Lond., Spec. Publ. 483, 19–37.

Sprain J, Renne PR, Vanderkluysen L, Pande K, Self S, Mittal T 2019 The eruptive tempo of Deccan volcanism in relation to the Cretaceous- Paleogene boundary; *Science* **363**, 866-870.

Tarling, D. H. (1983). Palaeomagnetism: principles and applications in Geology, Geophysics and Archaeology. New York: Chapman and Hall.

Tauxe, L. (2010). Essentials of Paleomagnetism. University of California Press. ISBN 978-0-520-26031-3.

van Hinsbergen DJJ et al. 2015 Dynamics of intraoceanic subduction initiation: 2. Suprasubduction zone ophiolite formation and metamorphic sole exhumation in context of absolute plate motions; *Geochemistry Geophysics Geosystems* **16**, 1771-1785 doi:10.1002/2015gc005745.

van Hinsbergen DJJ, Steinberger B, Doubrovine PV, Gassmöller R 2011 Acceleration and deceleration of India-Asia convergence since the Cretaceous: Roles of mantle plumes and continental collision; *Journal of Geophysical Research* **116**. doi:10.1029/2010jb008051.

Vandamme D, Courtillot V, Besse J, Montigny R 1991 Palaeomagnetism and age determinations of the Deccan Traps (India); results of a Nagpur– Bombay traverse and review of earlier work; *Reviews of Geophysics* **29**, 159–190.

Velasco-Villareal M, Urrutia-Fucugauchi J, Rebolledo-Vieyra M, Perez-Cruz L 2011 Paleomagnetism of impact breccias from the Chicxulub crater - Implications for ejecta emplacement and hydrothermal processes; *Physics of the Earth and Planetary Interiors* **186**, 154–171.

Venkateshwarlu M 2020 New paleomagnetic pole and magnetostratigraphy of the Cauvery Basin sediments, southern India; *J Earth Syst Sci* **129**, 222. https://doi.org/10.1007/s 12040-020-01476-z.

Wensink H 1973 Newer paleomagnetic results of the Deccan traps, India; *Tectonophysics* **17**, 41-59.